Deoxygenation of fatty acids for production of fuels and chemicals

Bartosz Rozmysłowicz

Laboratory of Industrial Chemistry and Reaction Engineering
Process Chemistry Centre
Department of Chemical Engineering
Åbo Akademi University
Turku/Åbo, 2014

Bartosz Rozmysłowicz

Born 1985 in Poznań, Poland

M.Sc. Eng. 2009,
Chemical Technology,
Poznań University of Technology,
Poland

Deoxygenation of fatty acids for production of fuels and chemicals

Bartosz Rozmysłowicz

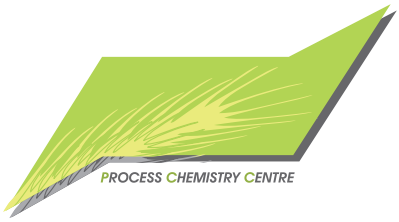

Laboratory of Industrial Chemistry and Reaction Engineering
Process Chemistry Centre
Department of Chemical Engineering
Åbo Akademi University
Åbo, Finland 2014

Supervised by

Professor Dmitry Yu. Murzin

Laboratory of Industrial Chemistry and Reaction Engineering
Process Chemistry Centre
Department of Chemical Engineering
Åbo Akademi University
Finland

Reviewers

Professor Hero Jan Heeres

Department of Chemical Engineering,
University of Groningen,
Nijenborgh 4, 9747 AG Groningen, The Netherlands

Professor Moti Herskowitz

Chemical Engineering Department,
Blechner Center for Applied Catalysis and Process Development,
Ben-Gurion University of the Negev,
Beer-Sheva 84105, Israel

Opponent

Professor Hero Jan Heeres

Department of Chemical Engineering,
University of Groningen,
Nijenborgh 4, 9747 AG Groningen, The Netherlands

ISBN 978-952-12-3102-5
Painosalama Oy – Turku, Finland 2014

Dla Justyny

PREFACE

This work was performed between 2010 and 2014 at the Laboratory of Industrial Chemistry and Reaction Engineering in the Department of Chemical Engineering at Åbo Akademi University. The research was a part of activities at Process Chemistry Centre (PCC), the centre of excellence funded by Åbo Akademi University.

The financial support from the Academy of Finland, Laboratory of Industrial Chemistry and Reaction Engineering, Rector of Åbo Akademi and YTK is gratefully acknowledged.

I would like to express my gratitude to Professor Dmitry Yu. Murzin and Professor Tapio Salmi for giving me the opportunity to work at the Laboratory of Industrial Chemistry and Reaction Engineering. Professor Murzin, thank you for your guidance, scientific advice and interesting discussions. I really appreciate that your office doors were always open for me.

I am deeply grateful to Docent Päivi Mäki-Arvela for her help and support throughout all these years. Moreover, I would like to thank Kari Eränen for his help and patience in the engineering side of this project. Also, I would like to thank Anton Tokarev for his help and valuable advices.

I would like to acknowledge all my collaborators: Atte Aho, Prof. Rasmus Fehrmann, Prof. Christopher Hardacre, Teuvo Kilpiö, Alexey Kirilin, Krisztián Kordás, Anne-Riikka Leino, Anders Theilgaard Madsen, Haresh Manyar, Prof. Andrey Simakov, Irina Simakova, Olga Simakova, Siswati Lestari and Johan Wärnå are acknowledged for their high contribution to my research work. Moreover, I would like to express my gratitude to all my co-workers from the Laboratory of Industrial Chemistry and Reaction Engineering who I encountered during PhD studies for their direct and indirect help and support.

I would like to thank my friends from the Laboratory of Industrial Chemistry and Reaction Engineering: Alexey, Anton, Atte, Cesar, Gerson, Ikenna, Olga and Pasi, without you this experience would not be the same. Thank you for the help when I needed it, interesting discussions and all the time we have spent together. Furthermore, I would like to express my gratitude to all of my Polish friends in Finland: Bartek, Marek, Michał, Milena, Patrycja, Paulina and Weronika. Thank you for all these years! Special thanks to Dorota and Grzegorz. From the beginning you were always there for me when I needed and you newer refuse to help – dzięki.

Finally, I would like to express my gratitude to my family, especially to my mother who always believed that I can achieve everything I dreamed of – dziękuję Mamo.

Last but not least, I would like to thank my wife Justyna for her unconditional love that we share together, for her support on every step on my scientific path and especially for her patience that she showed during writing process of this thesis. This is all thanks to you, without you my life would be meaningless – Kocham Cię Piękna.

ABSTRACT

The decreasing fossil fuel resources combined with an increasing world energy demand has raised an interest in renewable energy sources. The alternatives can be solar, wind and geothermal energies, but only biomass can be a substitute for the carbon–based feedstock, which is suitable for the production of transportation fuels and chemicals. However, a high oxygen content of the biomass creates challenges for the future chemical industry, forcing the development of new processes which allow a complete or selective oxygen removal without any significant carbon loss. Therefore, understanding and optimization of biomass deoxygenation processes are crucial for the future bio–based chemical industry. In this work, deoxygenation of fatty acids and their derivatives was studied over Pd/C and TiO_2 supported noble metal catalysts (Pt, Pt–Re, Re and Ru) to obtain future fuel components.

The 5 % Pd/C catalyst was investigated in semibatch and fixed bed reactors at 300 °C and 1.7–2 MPa of inert and hydrogen–containing atmospheres. Based on extensive kinetic studies, plausible reaction mechanisms and pathways were proposed.

The influence of the unsaturation in the deoxygenation of model compounds and industrial feedstock – tall oil fatty acids – over a Pd/C catalyst was demonstrated. The optimization of the reaction conditions suppressed the formation of by–products, hence high yields and selectivities towards linear hydrocarbons and catalyst stability were achieved.

Experiments in a fixed bed reactor filled with a 2 % Pd/C catalyst were performed with stearic acid as a model compound at different hydrogen–containing gas atmospheres to understand the catalyst stability under various conditions. Moreover, prolonged experiments were carried out with concentrated model compounds to reveal the catalyst deactivation.

New materials were proposed for the selective deoxygenation process at lower temperatures (~200 °C) with a tunable selectivity to hydrodeoxygenation by using 4 % Pt/TiO_2 or decarboxylation/decarbonylation over 4 % Ru/TiO_2 catalysts. A new method for selective hydrogenation of fatty acids to fatty alcohols was demonstrated with a 4 % Re/TiO_2 catalyst. A reaction pathway and mechanism for TiO_2 supported metal catalysts was proposed and an optimization of the process conditions led to an increase in the formation of the desired products.

REFERAT

Minskande resurser av fossila bränsletillgångar kombinerade med ett stigande globalt energibehov har ökat intresset för förnyelsebara energikällor. Möjliga alternativ är sol-, vind- och geotermisk energi, men endast biomassan kan ersätta kolbaserade råvaror, eftersom kemiska komponenter i biomassan lämpar sig för produktion av bränslekomponenter och kemikalier. Den höga syrehalten i biomassan utgör en stor utmaning för den kemiska industrin och tvingar fram en intensiv utveckling av nya processer vilka möjliggör en fullständig eller selektiv avspjälkning av syre utan att några som helst väsentliga kolförluster förekommer. Därför är en djupgående förståelse och optimering av syreavspjälkningen från biomassan ytterst viktig för en framtida biobaserad industri. I detta doktorsarbete studerades syreavspjälkning från fettsyror och fettsyraderivat på palladiumkatalysatorer och titandioxidburna ädelmetallkatalysatorer (platina, platina-renium och rutenium) med tanke på framställning av framtida bränslekomponenter.

En palladiumkatalysator studerades i en halvkontinuerlig reaktor och en kontinuerlig packad bäddreaktor vid 300 °C och ca 20 atmosfärs tryck. Experiment genomfördes under inerta och väterika atmosfärer. På basis av omfattande kinetiska studier föreslogs möjliga reaktionsmekanismer och reaktionsrutter.

Effekten av dubbelbindningar i vissa modellkomponenter och i industriell råvara – talloljefettsyror – demonstrerades för palladiumkatalysatorn. Optimering av reaktionsbetingelserna minimerade bildningen av biprodukter, varvid höga utbyten och selektiviteter av linjära kolväten uppnåddes och katalysatorn visade en god stabilitet.

Experiment i en packad bäddreaktor fylld med palladiumkatalysatorpartiklar genomfördes med stearinsyra som modellkomponent under olika väterika gasmiljöer för att bättre förstå katalysatorns stabilitet under varierande betingelser. Även långtidsexperiment genomfördes med koncentrerade modellkomponenter för att studera katalysatordeaktivering.

Nya katalytiska material föreslogs för selektiv syreavspjälkning vid lägre temperature (ca 200 °C), så att produktselektiviteten kunde styras för avspjälkningen (Pt/TiO_2-katalysator) och dekarboxylerings-dekarbonyleringsreaktionerna (Ru/TiO_2-katalysatorer). En ny metod demonstrerades för selektiv hydrering av fettsyror till alkoholer med hjälp av en Re/TiO_2-katalysator. Reaktionsrutter och –mekanismer för titandioxidbaserade metallkatalysatorer föreslogs. Optimering av processbetingelserna ledde till en utökad bildning av önskade produkter.

ABSTRAKT

Zmniejszające się zasoby paliw kopalnych oraz rosnące globalne zapotrzebowanie na energię wzbudziło zainteresowanie odnawialnymi źródłami energii. Alternatywą dla paliw kopalnych jest energia słoneczna, wiatrowa czy geotermalna. Jednakże tylko biomasa jest substytutem surowców na bazie węgla, który jest odpowiedni do produkcji paliw dla transportu czy substratów dla przemysłu chemicznego. Wysoka zawartość tlenu w biomasie stanowi wyzwanie dla przemysłu chemicznego, wymuszając rozwój nowych technologii umożliwiających całkowite lub selektywne usunięcie tlenu bez znaczącej utraty węgla. Dlatego też zrozumienie i optymalizacja procesów odtleniania biomasy ma kluczowe znaczenie dla przyszłości przemysłu chemicznego opierającego się na bazie biomasy. Celem tej pracy było badanie procesu deoksygenacji kwasów tłuszczowych i ich pochodnych na katalizatorach Pd/C jak również na TiO_2 domieszkowanym metalami szlachetnymi (Pt, Pt-Re, Re i Ru) w celu uzyskania paliw odnawialnych i związków chemicznych.

Badania nad katalizatorem węglowym o zawartości 5 % palladu przeprowadzone zostały w reaktorze półokresowym w temperaturze 300 °C oraz atmosferze zawierającej argon bądź wodór o ciśnieniu 1,7–2 MPa. Na podstawie szeroko zakrojonych badań kinetycznych zaproponowano potencjalne mechanizmy i ścieżki reakcji.

Następnie zbadano wpływ nienasyconych kwasów tłuszczowych na wydajność procesu odtleniania z wykorzystaniem katalizatora palladowego. Badania przeprowadzono bazując na modelowych związkach oraz mieszaninach pochodzenia przemysłowego (olej talowy). Dzięki optymalizacji warunków reakcji, ograniczono powstawanie produktów ubocznych, tym samym zwiększając stabilność katalizatora. W rezultacie otrzymano wzrost wydajności procesu oraz selektywności względem liniowych węglowodorów.

W celu uzyskania informacji na temat zależności stabilności katalizatora od kompozycji fazy gazowej, wykonano szereg doświadczeń z kwasem stearynowym przy użyciu reaktora przepływowego ze złożem wypełnionym 2 % Pd/C. Dodatkowo przeprowadzone zostały długotrwałe eksperymenty ze skoncentrowanymi związkami modelowymi, które były źródłem wiedzy na temat dezaktywacji katalizatora.

W świetle dokonanych badań zaproponowano innowacyjne katalizatory do selektywnego procesu odtleniania w niższych temperaturach (~200 °C). Poprzez depozycje różnych metali szlachetnych, otrzymano wysokie selektywności w kierunku hydrodekarboksylacji, przez stosowanie 4 % Pt/TiO_2, lub dekarboksylacji/dekarbonylacji, używając 4 % Ru/TiO_2. Ponadto, przedstawiono nowy sposób selektywnego uwodornienia kwasów tłuszczowych do alkoholi tłuszczowych za pomocą 4 % Re/TiO_2. W oparciu o otrzymane wyniki zaproponowano mechanizmy i ścieżki reakcji przy użyciu różnych katalizatorów zawierających metale szlachetne osadzone na TiO_2. Optymalizacja warunków procesu zwiększyła jego selektywność w kierunku pożądanego produktu.

List of publications

I. Bartosz Rozmysłowicz, Päivi Mäki-Arvela, Dmitry Yu. Murzin, *Fatty Acids-Derived Fuels from Biomass via Catalytic Deoxygenation*, Biomass Conversion, Springer (2012) 199-220
Contribution: wrote and edited the article

II. Bartosz Rozmysłowicz, Päivi Mäki-Arvela, Anton Tokarev, Anne-Riikka Leino, Kari Eränen, Dmitry Yu. Murzin, *Influence of hydrogen in catalytic deoxygenation of fatty acids and their derivatives over Pd/C,* Ind Eng Chem Res, 51 (2012) 8922
Contribution: performed the experiments, wrote and edited the article

III. Irina Simakova, Bartosz Rozmysłowicz, Olga Simakova, Päivi Mäki-Arvela, Andrey Simakov, Dmitry Yu. Murzin, *Catalytic deoxygenation of C18 fatty acids over mesoporous Pd/C catalyst for synthesis of biofuels*, Top Catal 54 (2011) 460
Contribution: performed most of the experiments, contributed to writing of the article

IV. Bartosz Rozmysłowicz, Päivi Mäki-Arvela, Siswati Lestari, Olga A. Simakova, Kari Eränen, Irina L. Simakova, Dmitry Yu. Murzin, Tapio Salmi, *Catalytic deoxygenation of tall oil fatty acids over a palladium-mesoporous carbon catalyst: a new source of biofuels*, Top Catal 53 (2010) 1274
Contribution: performed experiments, wrote and edited the article

V. Päivi Mäki-Arvela, Bartosz Rozmysłowicz, Siswati Lestari, Olga Simakova, Kari Eränen, Tapio Salmi, Dmitry Yu. Murzin, *Catalytic deoxygenation of tall oil fatty acid over palladium supported on mesoporous carbon*, Energ Fuel, 25 (2011) 2815
Contribution: performed the experiments, contributed to writing and editing of the article

VI. Anders Theilgaard Madsen, Bartosz Rozmysłowicz, Irina L. Simakova, Teuvo Kilpiö, Anne-Riikka Leino, Krisztián Kordás, Kari Eränen, Päivi Mäki-Arvela, Dmitry Yu Murzin, *Step changes and deactivation behavior in the continuous decarboxylation of stearic acid,* Ind Eng Chem Res, 50 (2011), 11049
Contribution: contributed to experiments and editing of the article

VII. Anders Theilgaard Madsen, Bartosz Rozmysłowicz, Päivi Mäki-Arvela, Irina L. Simakova, Kari Eränen, Dmitry Yu Murzin, Rasmus Fehrmann, *Deactivation in continuous deoxygenation of C18-fatty feedstock over Pd/Sibunit,* Top Catal, 56 (2013) 714
Contribution: contributed to experiments and editing of the article

VIII. Bartosz Rozmysłowicz, Alexey Kirilin, Atte Aho, Haresh Manyar, Christopher Hardacre, Johan Wärnå, Tapio Salmi, Dmitry Yu. Murzin, *Selective hydrogenation of fatty acids to alcohols over highly dispersed ReO_x/TiO_2 catalyst,* (Submitted)
Contribution: performed the experiments, wrote and edited the article

List of related publications

1) *1st International Conference Catalysis for Renewable Sources: Fuel, Energy, Chemicals*, 28 June – 2 July 2010 (oral presentation), Tsars Village, St. Petersburg, Russia

2) *Catalysis in Multiphase Reactors CAMURE-8 and International Symposium on Multifunctional Reactors ISMR-7,* 22–25 May 2011 (poster presentation), Naantali, Finland

3) *The 15th Nordic Symposium on Catalysis*, 10 - 12 June 2012 (poster presentation), Mariehamn, Åland

4) *15thInternational Congress on Catalysis 2012*, 1–6 July 2012 (poster presentation), Munich, Germany

5) *CAT4BIO, an international conference on "Advances in catalysis for biomass valorization"*, 8–11 July 2012 (oral presentation), Thessaloniki, Greece

Content

1. Introduction

1.1 World energy demand

World crude oil reserves, according to OPEC[1], are at a level of 1478.2 billion barrels. In 2013, the daily world consumption reached 90.4 mb/d (million barrels per day) with the forecast of an increase by 1.2 mb/d and 1.3 mb/d in the following two years, respectively[2]. It can therefore be estimated that the world has roughly 45 years before all the oil will be consumed. This is based on an assumption that the world crude oil consumption will be maintained at the same level. However, the consumption of crude oil is forecasted to increase by 19 mb/d to reach a level 109 mb/d by 2035[3]. While a noticeable decrease in the consumption will be observed in the OECD countries, the non-OECD states will contribute to the consumption increase in both transport and industry by 16.6 mb/d and 8.7 mb/d, respectively. This trend will be caused mainly by the economic and population growth of countries such as China and India, where an increase in the wealth will be followed by an increase of the energy demand, particularly in the transportation sector. The unavoidable depletion of the fossil fuel reserves creates an urgent need for the development of the new technologies for the production of fuels and chemicals based on renewable sources.

Liquid fuels are mainly used in the transportation sector. Although, it is estimated that in the near future, oil will have the main share of the market (87 % by 2035) biofuels production will grow gradually by 1.9 mb/d until 2035[3]. In numerous countries legislation measures have recently been taken to increase biofuels share in transportation fuels. A good example is the European Union where the level of the biofuels within the fuel mix has to reach 10 % both in gasoline and

diesel by 2020[4]. This goal creates a driving force for both scientists and industry to develop new processes which cope with production increase, while maintaining the required by legislation[4] 60 % decrease in the carbon dioxide generation for biofuels in comparison to fossil fuels.

1.2 Deoxygenation of biomass

Biomass consists of high amounts of oxygen, for instance, in wood biomass it can vary between 40-45 %. Similarly, fuels obtained from biomass contain a high oxygen–to–carbon ratio which influences its burning properties i.e. the heating value [MJ/kg]. Therefore, to improve the fuel properties, oxygen has to be removed, which can be achieved by deoxygenation. Upgrading of biofuels via deoxygenation is mainly used for fats[5]. The process itself can be divided into hydrodeoxygenation (HDO) and decarboxylation-decarbonylation processes (DCO). Hydrodeoxygenation requires the presence of hydrogen to reduce oxygenates species, while DCO removes the whole functional group by the carbon–carbon bond cleavage, releasing CO or CO_2.

Deoxygenation can be used for direct transformation of renewable feedstock to diesel range hydrocarbons. The most common example is the conversion of vegetable oils extracted from plants to produce high quality diesel[6–9]. This process can also use residues from the food industry (e.g. animal fats[5] or waste cooking oil[10]) or from pulp and paper industries **[IV, V]**. Moreover, transformation of bio-oils was proposed as a way for upgrading final fuel product properties [11].

Hydrodeoxygenated fats and bio-oils show superior properties in comparison with conventional biodiesel (fatty acid methyl ester – FAME) produced via transesterification or non-treated bio-oil obtained from fast pyrolysis (*Table 1*). The removal of oxygen gives biofuel properties similar to those of conventional fossil fuels, which is especially important for transportation fuels, in which biodiesel is often blended with conventional diesel components.

Table 1. Fuel property comparison between fossil diesel, FAME, HDO diesel, oil from pyrolysis and hydrodeoxygenated bio-oil. Adapted from ref. [12,13].

	Units	Fossil Diesel	FAME Biodiesel	HDO Diesel	Flash Pyrolysis Bio-Oil	HDO Bio-Oil
Cetane Number	–	50	45–72.7	80–99	–	–
RON	–	–	–	–	–	77
Heating Value	[MJ/kg]	42–45	37.1–40.4	42–44	22.6	42.3–45.3
Oxygen	[wt.%]	0	10.7–13.2	0	28-40	0–0.7
Sulfur	[mg/kg]	12	0–0.012	10	–	50
Moisture	[mg/kg]	0.5	28.5–500	42–95	2–3 (*10^5)	1–8
Aromatic/Aliphatic	–	–	–	–	22.6	42.3-45.3
Density	[g/ml]	0.85	0.855–0.9	0.77–0.83	1.1–1.3	0.79–0.93
Viscosity (40 °C)	[cSt]	2.71	3.89–7.9	2.5–4.15	15–35	1.0–4.6 (23 °C)
Flash Point	[°C]	52–136	96–188	68–120	–	–

1.3 Hydrodeoxygenation over sulfided bimetallic catalysts

Hydrodeoxygenation of fats is widely used on an industrial scale for the production of diesel–range hydrocarbons. The first plant was constructed by Neste Oil in Finland with a capacity of 0.17 Mt in 2007. Since then, three new units have been constructed (Porvoo, Rotterdam and Singapore) giving total capacity of 2 Mt/a[5]. The brand announced by Neste Oil for this fuel is NExBTL (Next generation Biomass-To-Liquids) although synonyms such as “green diesel” or “renewable diesel” are used as equivalents [5].

The process is operated under elevated hydrogen pressure, typically between 3.5 MPa[14] to 15 MPa[15] with temperature range from 250–360 °C[16]. The most commonly used catalysts are bimetallic NiMo[6,17] and CoMo[18,19] sulfides supported on Al_2O_3. The catalyst has to be sulfided to achieve a good activity at relatively low temperatures because non–sulfided NiMo/Al_2O_3 exhibits a low activity and selectivity towards hydrocarbons[17,20].

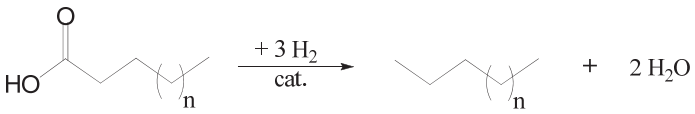

Figure 1. Hydrodeoxygenation of fatty acids.

In hydrodeoxygenation, the carboxylic group is reduced to its corresponding hydrocarbon (*Figure 1*). However, decarboxylation and decarbonylation can proceed also over a sulfided catalyst depending on the ratio between the metals used for catalyst preparation (*Figure 2*). In the case of a sulfided $NiMo/Al_2O_3$ catalyst Ni promotes decarboxylation/decarbonylation, while Mo has a high selectivity towards the hydrogenation of the carboxylic group[21]. Therefore, hydrodeoxygenation has to be treated as a process, in which the reduction of the carboxylic group takes place predominantly but not exclusively.

1.4 Decarboxylation/decarbonylation over supported noble metal catalysts

Decarboxylation/decarboxylation of fatty acids is an alternative process to hydrodeoxygenation of fats and free fatty acids over sulfided catalysts. The reaction occurs over a supported metal catalyst yielding (n-1)–carbon alkanes and CO_2 or CO and water (*Figure 2*). The advantage of this method is in a decreased use of hydrogen, because hydrogen is principally not needed for this reaction. Moreover, sulfidation of the catalyst, needed for NiMo and CoMo, is not required.

The reaction is performed at around 300 °C and 0.6 MPa – 2 MPa in an inert[22–24] or hydrogen–containing atmosphere[25,26]. The most active catalysts for deoxygenation were found to be Pd and Pt while some other metals such Mo, Ni, Ru, Rh, Ir and Os showed lower activity[27].

Palladium supported over active carbon showed superior activity and selectivity towards the decarboxylation yielding stearic acid and CO_2 in comparison to platinum on active carbon which was more selective towards decarbonylation yielding high amounts of CO[27].

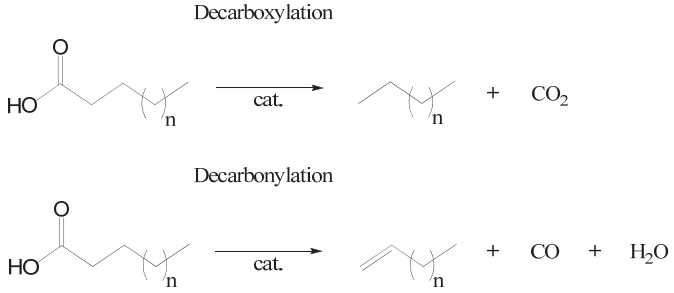

Figure 2. Decarboxylation and decarbonylation reaction.

Although the active metal was selected, the search remains for the best catalyst support. Noble metals supported over mesoporous materials have turned out to be active in decarboxylation[23,28]. Moreover, bifunctional catalysts comprised of an active metal site and a reactive support have been proposed, i.e. acidic SAPO–31[29] which enhances the skeletal isomerization of products or basic MgO[27] allowing the condensation of fatty acids to C_{35} ketones. Furthermore, a Ni/ZrO_2 catalyst was proposed which exhibits a high activity for the deoxygenation of fats due to the oxygen vacancies in ZrO_2[30].

1.5 Selective hydrogenation of fatty acids

Fatty alcohols are important bio–based chemicals which are used as non–ionic surfactants and emulsifiers, emollients and thickeners in alimentary and cosmetic industry and the substrate for production of other surface-active materials such as alkylamines and alkylsulfates[31]. The current world production capacity reaches 3.35 Mt/a, with an estimated global demand growth (2012–2017) of 3.2 %/a[32]. Fatty alcohols are mainly produced through catalytic hydrogenation of fatty acids and its derivatives (*Figure 3*). In traditional processes, methyl esters are hydrogenated over Cu-Cr-based[31] catalysts with a high selectively towards alcohols. However, due to the low reactivity of the carboxyl group, elevated temperatures (200–300 °C) and hydrogen pressures (20–30 MPa) have to be applied. Moreover, chromium catalysts are not environmentally friendly due to the release of hazardous chromium compounds into the environment.

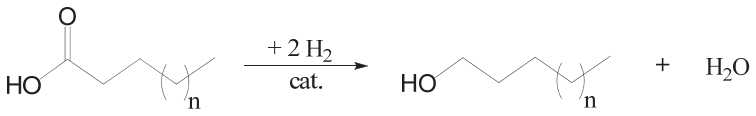

Figure 3. Selective hydrogenation of fatty acids to alcohols.

Noble metal catalysts such as Ru or Pt were reported to be active in selective hydrogenation of fatty acids. Many kinds of Ru-based catalyst have been studied[33] from which bimetallic Ru-Sn/Al_2O_3[34] has shown the highest selectivity towards fatty alcohols (250 °C; 5.6 MPa). In addition, a change of the support in Ru-Sn catalysts from Al_2O_3 to TiO_2 has increased the activity and selectivity which can be ascribed to Ru-Ti metal support interactions[35]. Similar properties were observed with a Pt/TiO_2 catalyst[36] as hydrogenation of fatty acids to alcohols was performed at low temperatures (110–150 °C) and hydrogen pressures (2 MPa) with a selectivity of 90–93 %.

Selective hydrogenation of fatty acids to alcohols has been investigated over rhenium-based catalysts. The reaction of decanoic acid was performed over Re_2O_7 at 10 MPa of hydrogen and 130 °C resulting in a low conversion and selectivity (74%) towards 1-decanol[37]. Moreover, it was shown that the addition of OsO_4 to form a bimetallic Re-Os[37] catalyst increased the rate and selectivity to 84 %. Furthermore, Re and bimetallic Re-Sn deposited over ZrO_2 and Al_2O_3 were studied at 250 °C and 5.6 MPa of hydrogen pressure in the hydrogenation of oleic acid. The Re/Al_2O_3 catalyst afforded the highest selectivity to alcohols, reaching 58 %[38].

2. Experimental section

2.1 Materials

2.1.1 Substrates

In most of the reactions, the substrate (the reactant) was diluted before the reaction by dodecane (Sigma-Aldrich, 99 %) [**III-VIII**] or hexadecane (Aldrich, 99 %). Depending on the research target, different substrates were used: stearic acid (Merck; 97 %) [**III, VI-VIII**], octadecanol (Aldrich; 99 %) [**II**], oleic acid (Fluka, 90 %) [**III**], linoleic acid (Fluka; 99 %) [**III**], lauric acid (Sigma; 99 %) [**II**], lauric aldehyde (SAFC; ≥95 %) [**II**], lauryl alcohol (Fluka; ≥98.5 %) [**II**], tall oil fatty acids TOFA (Forchem, neat) [**IV, V**], ethyl stearate (SAFC; ≥97 %) [**VII**] and tristearin (Aldrich; 65 % - stearic acid; 35 % palmitic acid - content) [**VII**]. The chemical analyses were performed with N,O-Bis(trimethylsilyl)trifluoroacetamide (BSTFA) (Sigma-Aldrich, ≥99 %), chlorotrimethylsilane (TMCS) (Sigma-Aldrich ≥99 %) and Pyridyne (Sigma-Aldrich anhydrous ≥99.8 %).

2.1.2 Catalysts

The deposition-precipitation method was used for the preparation of 1 [**III-V**] and [**II**] 5 wt% Pd catalyst on a mesoporous carbon Sibunit. The sibunit carbon was crushed and sieved to obtain particles below 70 μm to suppress internal mass transfer limitations in the catalyst pores. Prior to the Pd deposition, the support was treated with 5 wt% HNO_3 overnight and thereafter dried at

80 °C for 8 h. The Pd precursor, H_2PdCl_4 was hydrolyzed in aqueous solution by adding Na_2CO_3 with a 1:21 molar ratio. The formed polynuclear hydroxycomplexes of Pd (II) were deposited onto the carbon surface[39,40]. After a complete Pd adsorption on the carbon surface, the catalyst was filtered and washed with deionized water until no Cl^- ions could be detected in the washing solution. Thereafter, the catalyst was calcined in air at 200 °C for 2 h. The same preparation method was used for preparation the 2 wt% Pd supported catalyst beads (1.5–2 mm) [**VI, VII**].

TiO_2 (P90) supported noble metal Pt, Re and Ru catalysts were prepared by the incipient wetness impregnation techniques [**VIII**]. An appropriate mass of the precursor was diluted with de–ionised water (18 MΩ) of a volume equal to the pore volume of the support. The solution was added to the support in three portions of equal volumes with stirring after each addition until thoroughly mixed. The product was dried at 120 °C for 12 h followed by calcination at 500 °C for 4 h. The bimetallic PtRe catalyst was prepared by sequential incipient wetness impregnation (S.I.). In the case of sequential impregnation, following the deposition of one metal, the catalyst was dried and calcined before the process was repeated for the second metal. After this deposition, the catalyst was again dried and calcined.

2.2 Catalyst characterization techniques

2.2.1 Carbon monoxide chemisorption

The palladium dispersion was measured by pulse CO chemisorption with the Autochem 2910 apparatus (Micromeridics). Prior the analysis, the catalyst was dried overnight in the oven at 100 °C. Thereafter, the catalysts were reduced under a hydrogen flow at 200 °C (Pd [**II-V**]), 250 °C (Pt), 300 °C (Ru) and 400 °C (Re [**VIII**]), and cooled to 25 °C, where pulses of 10 % CO were injected until no more adsorption was observed.

2.2.2 Transmission electron spectroscopy (TEM)

The metal particle size distribution was measured by high resolution transmission electron microscopy LEO 912 Omega (voltage 120 kV) [**II-VII**] and JEM-1400 Plus (voltage 120 kV)

[VIII]. Histograms of the particle size distribution were obtained by counting at least 100 particles on the micrographs for the sample. The catalysts before the analysis were reduced for 2 h at: 200 °C – Pd, 250 °C – Pt and 400 °C – Re.

2.2.3 Nitrogen physisorption

Pore volume and specific surface area measurements were conducted with a physisorption Sorptometer 1900 apparatus from Carlo Erba with liquid nitrogen at 77 K. The specific surface areas were calculated from the N_2 adsorption-desorption isotherms using the Brunauer-Emmett-Teller (BET) equation [**II–VIII**]. The pore size distribution was obtained from the Dollimore-Heal correlation.

2.2.4 X-ray diffraction (XRD)

The mean Pd particles diameter based on the particle volume were calculated with the Scherrer formula from powder diffractograms obtained on a Siemens D5000 X-ray powder diffractometer [**VI**].

2.2.5 X-ray photoelectron spectroscopy (XPS)

The Re/TiO_2 catalyst [**VIII**] was reduced at atmospheric pressure and at 0.5 MPa in hydrogen. The fresh catalyst was transported under acetone to a glovebox where it was filtrated and dried at room temperature in an inert atmosphere. Whereas the spent catalyst, was transported submerged in the reaction mixture to the glovebox. In an inert atmosphere, the catalyst was washed with acetone and dried at room temperature. All catalysts were brought to XPS in sealed containers. During insertion into the XPS the catalyst was in contact with air for less than 2 min.

A Perkin-Elmer PHI 5400 spectrometer with a Mg Kα X-ray source operated at 14 kV and 200 W was used in the XPS-analysis of the samples. The pass energy of the analyzer was 17.9 eV and the energy step 0.05 eV. The binding energy calibration was based on the Ti $2p_{3/2}$ peak at 458.8 eV. The sensitivity factors used in the quantitative analysis for O1*s*, Ti$2p_{3/2}$, Re4*f* and C1*s* were 0.711, 1.334, 3.961 and 0.296, respectively.

2.2.6 Temperature programmed reduction (TPR)

Prior to the analysis, an aliquot 50 mg of non–reduced catalyst was kept in the oven at 100 °C overnight. Temperature programmed reduction (TPR) was performed in Autochem Micromeritics 2910 using 5 % H_2 in Ar. The temperature ramp was 10°C/min to 500 °C [**VIII**].

2.2.7 Temperature programmed desorption (TPD)

Temperature programmed desorption (TPD) was performed in the Autochem Micromeritics 2910 equipment. Ammonia and CO_2 were used for the determination of acid and basic sites, respectively. The sample was at first kept in a helium atmosphere at 400 °C for 1 h, then cooled to 100 °C in the case of NH_3 TPD and 30 °C in the case of CO_2 TPD. Afterwards, the adsorbate was introduced to the sample surface for 30 min. Subsequently, the catalyst was flushed with an inert gas for 30 min after which the analysis was started. The temperature ramp was 10 °C/min up to 700 °C for NH_3 and 600 °C (CO_2) where the sample was kept for 1 h. Before the adsorption, the catalyst was reduced *in situ* under hydrogen at 250 °C (Pt, PtRe and Ru) and 400 °C (Re) for 2 h [**VIII**].

2.2.8 Inductively Coupled Plasma – Optical Emission Spectroscopy

The metal content of the catalyst was determined by Inductively Coupled Plasma (ICP) by using Optical Atomic-Emission Spectrometer Optima 4300 DV. Prior to the analysis, catalysts were dissolved in a microwave oven by an acid mixture [**II–VIII**]. Moreover, an analysis of the post-reaction mixture was performed [**VI**] to check the catalyst leaching.

2.2.9 Laser-ablation inductively coupled plasma mass spectrometry

The active metal distribution of active metal in fresh catalyst beads was investigated by laser-ablation inductively coupled plasma mass spectrometry (LA-ICP-MS), with a New Wave UP-213 laser ablation system and a Perkin-Elmer ICP-MS Sciex Elan 6100 DRC Plus system. A number of catalyst beads were cut in half and fixed in an epoxy glue for the measurements [**VI**].

2.3 Experimental procedures

2.3.1 Semibatch reactor

Kinetic and catalyst screening experiments were performed in a 300 ml semi-batch reactor autoclave coupled to a heating jacket and a condenser (*Figure 4*). The experimental temperature was set at 300–350 °C for Pd/C catalysts and 180–220 °C for Pt, Re, Pt-Re and Ru catalysts supported on TiO_2. The atmosphere in the reactor was 100 % Ar [**II**], 1 vol. % H_2 in Ar [**III–V**], 5 vol. % H_2 in Ar [**III**], 100 % H_2 [**II, IV, V, VIII**]. The reaction total pressure was 1.7 MPa [**III–V**], 2 MPa [**II**] and 2–4 MPa **[VIII**]. The flow (30 ml/min) was controlled by Brooks 58505S pressure controller and Brooks 5866 flow controller. The reactant mass 1 g [**II**], 2 g [**III**] or 4.5 g [**III–V**] was dissolved in 100 ml, 70 ml and 100 ml of the solvent, respectively, at 60 °C. Subsequently, the reaction mixture was injected to a pre–reactor where air was removed by the inert gas.

Prior to the experiments, the catalyst (100 mg [**II, III, VIII**]; 500 mg [**III–V**]; 1.4 g [**III**]) was reduced *in situ* in pure hydrogen at a 0.5 MPa pressure. The reduction temperature and time were varied depending on the catalyst: Pd/C for 1 h at 60 °C [**III–V**] and 200 °C [**II**]; Pt/TiO_2 for 2 h at 250 °C; Re/TiO_2 for 2 h at 400 °C; $PtRe/TiO_2$ for 2 h 250 °C; Ru/TiO_2 for 2 h 200 °C. In the experiments in an inert atmosphere, the catalyst was flushed after the reduction with argon for 0.5 h, at the reaction temperature, to remove all the remaining hydrogen from the reactor system. In the experiment with a non-reduced Re/TiO_2, the catalyst was heated to the reaction temperature in the inert gas atmosphere and the injection of hydrogen and the reaction mixture occurred simultaneously. The stirring speed during the reaction was kept at 1200 rpm to suppress external mass transfer limitations. Samples were periodically withdrawn from the reactor during the reaction.

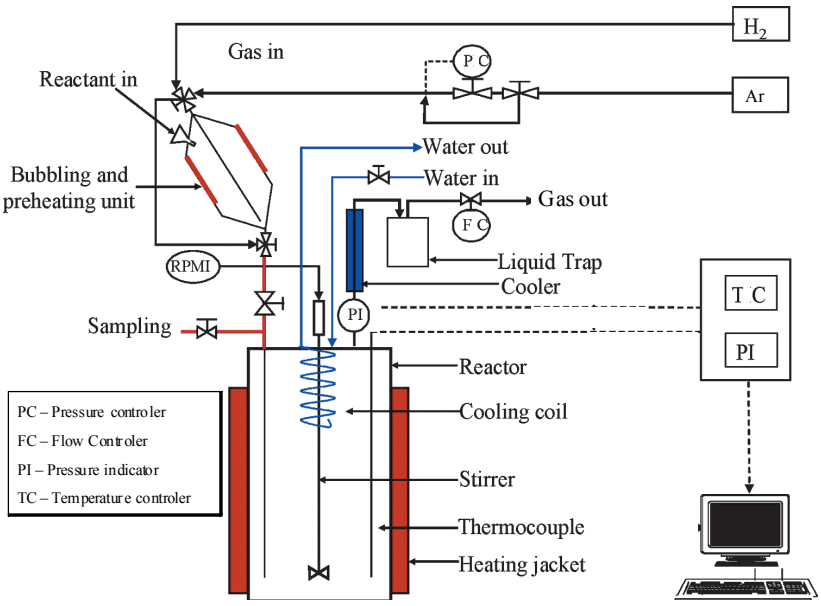

Figure 4. Semibatch reactor system. Adapted from:[24].

2.3.2 Continuous fixed bed reactor

A tubular fixed bed reactor of 18 cm height and 1.58 cm inner diameter (volume = 35.1 ml) was loaded from the bottom up with a small layer of quartz wool, followed by 6 ml of quartz sand of 0.2–0.8 mm diameter and a layer of quartz wool. The catalyst bed of 10 g (volume uptake = 19.0 ml) of 2 % Pd/Sibunit was loaded into the reactor. Thereafter, a layer of quartz wool, 4 ml of quartz sand, and another layer of quartz wool were introduced. A thermocouple was fixed at the center of the catalyst bed. The reactor was purged for 16 h at 20 bar with Ar at room temperature. The catalyst was activated in 5 % H_2/Ar at 2 MPa at temperature 150 °C for 1 h, and then heated at 10 °C/min to the reaction temperature of 300 ^{o}C. Reactions were performed in either in pure Ar or in a mixture of 5% H_2/Ar at 42 ml/min and with a flow of either pure stearic acid or 10 wt% stearic acid in n-dodecane, both at 0.075 ml/min [**VI**]. The feed vessel was heated at 90^{o}C, and the pump and inlet piping were maintained at 100^{o}C during experiments with pure stearic acid (*Figure 5*). Trace gas impurities (e.g., molecular oxygen) were expelled from the feed vessel by continuous purging of 20 ml/min nitrogen gas through the stearic acid.

For studying the catalyst deactivation during the deoxygenation process [**VII**], before each experiment, the reactor was loaded at the bottom with a layer of quartz wool, then 6 ml of quartz sand and a layer of quartz wool. In the middle of the reactor, the catalyst bed was placed of totally 10 g of 2 % Pd supported on Sibunit, divided into five equal layers of 2 g each, separated by a layer of quartz wool. The liquid feed consisted of either stearic acid, ethyl stearate or technical tristearin. The gas flow was supplied at 2 MPa, first using 5 % H_2/Ar at 42 ml/ min and after 75 h (stearic acid: 96 h) time-on-stream (TOS) the gas flow was switched to pure Ar and the reaction was continued for another 75 h (stearic acid: 54 h).

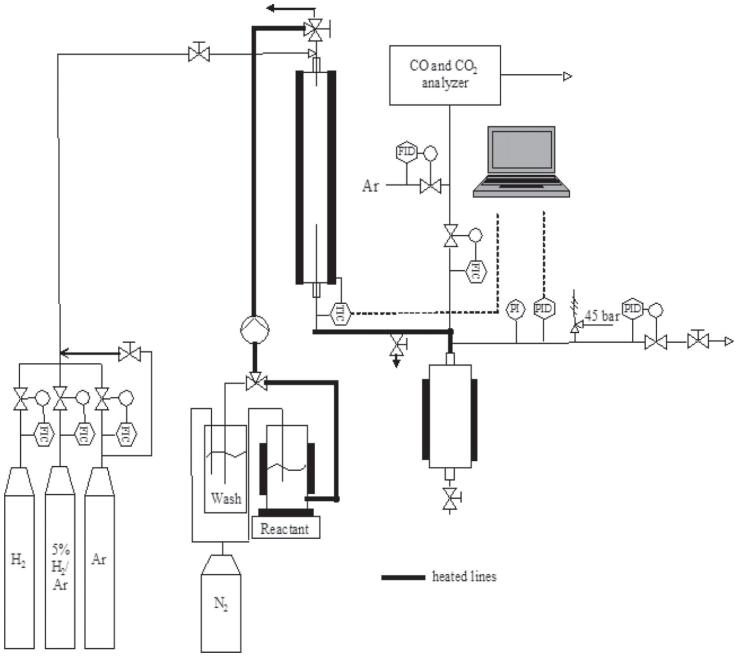

Figure 5. Continuous trickle bed reactor flowsheet. Adapted from:[41].

2.4 Product analysis

2.4.1 Liquid–phase analysis

Analysis of the liquid phase was performed with gas chromatograph (HP 5890) equipped with a ZB-5 Inferno column (30 m, 0.32 mm, 0.1 μm). Samples for analysis were prepared by mixing

0.1 ml of reaction mixture with 0.1 ml of silylation agent (BSTFA) 0.1 ml of TMCS, 0.05 ml of eicosane dissolved in dodecane (1 mg/ml) as an internal standard and 1 ml of pyridine. Thereafter, samples were left in the oven at 70 °C for 1 h to ensure proper silylation before injection to the GC. The same sample preparation procedure was performed before qualitative analysis in GC-MS (GC-6890N, MS-5973) with the chromatographic column DB-PETRO (100 m, 0.25 mm, 0.5 μm). In the reactions with neat substrate [**VI, VII**], the sample (~0.1 g) prior to analysis was dissolved in 4 ml of dodecane and 0.1 ml of this solution underwent silylation. The analysis of tristearin were performed on 7890A Network HP Agilent equipment

Size exclusion chromatography (SEC) was performed to determine fatty acids polymers in the post-reaction mixture [**III**]. The SEC system has three different columns: Jordi Protection column, Earth Igel DVB500A (7.8 mm x 300 mm), TSK G3000HHR (7.8 mm x 300 mm) and the LT–ELS detector (Low Temperature Evaporative Light Scattering Detector)

The neat tall oil fatty acid was analyzed for Cl, P and S content by ICP–OES and ion chromatography after previous microwave digestion in a mixture of 60 % nitric acid and 30 % hydrogen peroxide.

2.4.2 Gas–phase analysis

In experiments with a semibatch reactor [**II**], the gas–phase analysis was performed with a mass spectrometer (Omnistar GSD 300, Balzers Instruments) coupled to the reactor outlet as well as with a Micro GC (Agilent 3000) instrument. The mass spectrometer was calibrated prior to each experiment with a calibration mixture of 5 mol% hydrogen, 0.5 mol% CO and 1 mol% CO_2 in argon.

For the Micro GC system, each gas sample was analyzed 10 times to ensure a correct peak integration. The instrument was calibrated for numerous gases, including hydrogen, CO, CO_2, and light hydrocarbons. The samples for Micro GC were collected in 50 ml bottles from the reactor outlet immediately after taking the liquid sample.

In the experiments with the continuous trickle bed reactor [**VI, VII**], the gases were purged continuously through a pressure reduction controller, and a part of the gas stream was diluted in He and analyzed for the presence of CO and CO_2 on a Siemens ULTRAMAT 6 online IR analyzer.

3. Results and discussion

3.1 Catalyst characterization

The deoxygenation studies were performed over palladium supported on carbon [**II–VII**] and over various metal supported on TiO_2 [**VIII**]. The specific surface areas of the catalysts were measured before and after the metal deposition (*Table 2*). In all the carbon–based catalysts the surface area and pore volume decreased after the metal deposition on the surface. The titania–based catalysts exhibited a decrease of the surface area, however, their pore volumes slightly increased after the deposition.

With all of the catalysts, the deposition efficiency was very high, as the obtained metal loadings were very close to the desired values which was confirmed by ICP–OES. The metals in all of the catalysts were well dispersed on the support surface which ensured high activities. The nanoparticles of noble metals were below 3 nm for the powder catalysts and 6.7 nm for the catalyst beads [**VI–VII**]. This difference is caused by the egg-shell deposition of the active metal on Sibunit beads which was confirmed by laser-ablation analysis. Palladium was deposited on the outer layer (10 μm) of the beads and only a small part of the support was enriched with the noble metal. Therefore, a local concentration of palladium is higher which leads to a larger nanoparticle size in comparison with the powder catalyst.

Table 2. Specific surface area of catalysts and metal content, dispersion and particle size.

	TEM	CO chemisorption		Specific surface area	Pore volume	Nominal metal loading
		metal dispersion	Average particle size			
	nm	%	nm	m^2/g	ml/g	wt %
1 % $Pd/C_{(A)}$	1.9	67[a]	1.7[a]	236	–	0.98
1 % $Pd/C_{(B)}$	2.6	38[a]	2.7[a]	379	0.987	0.99
2 % $Pd/C_{(C)}$[d]	6.7	15[a]	7.2	361	0.873	–
4 % $Pd/C_{(D)}$	1.7	45[a]	2.4[a]	450	–	–
5 % $Pd/C_{(E)}$	2.4	47[a]	2.4[a]	357	0.62	5.1
4 % Pt/TiO_2	2.0	26[b]	4[b]	83	0.20	4
4 % Re/TiO_2	0.9	~100[c]	~1[c]	63	0.22	3.8
4 % Ru/TiO_2	–	7	20	–	–	–
4 % Pt – 4 % Re/TiO_2	–	–	–	53	0.17	4.3–3.5
$C_{(C)}$[d]	–	–	–	504	1.23	–
$C_{(E)}$	–	–	–	399	0.66	–
TiO_2	–	–	–	108	0.18	–

[a] stoichiometry of CO/Pd – 0.5; [b] stoichiometry of CO/Pt – 1; [c] stoichiometry of CO/Re for oxide Re^{4+} and Re^{6+} species – 0.35 [42]; [d] sibunit beads 1.5–2 mm; A–C – different Sibunit carbon materials.

The average, metal nanoparticle diameter was calculated based on TEM images and CO chemisorption measurements. A comparison is presented in *Table 2*. The general the agreement between the two methods was very good. A slight difference between the results can be attributed to the uncertainty in the assumed adsorption stoichiometry of CO on the metal. Therefore, an average particle size obtained by fitting the particle size distribution histograms from the TEM images is closer to the reality. The histograms and images of the catalysts are displayed in *Figure 6*.

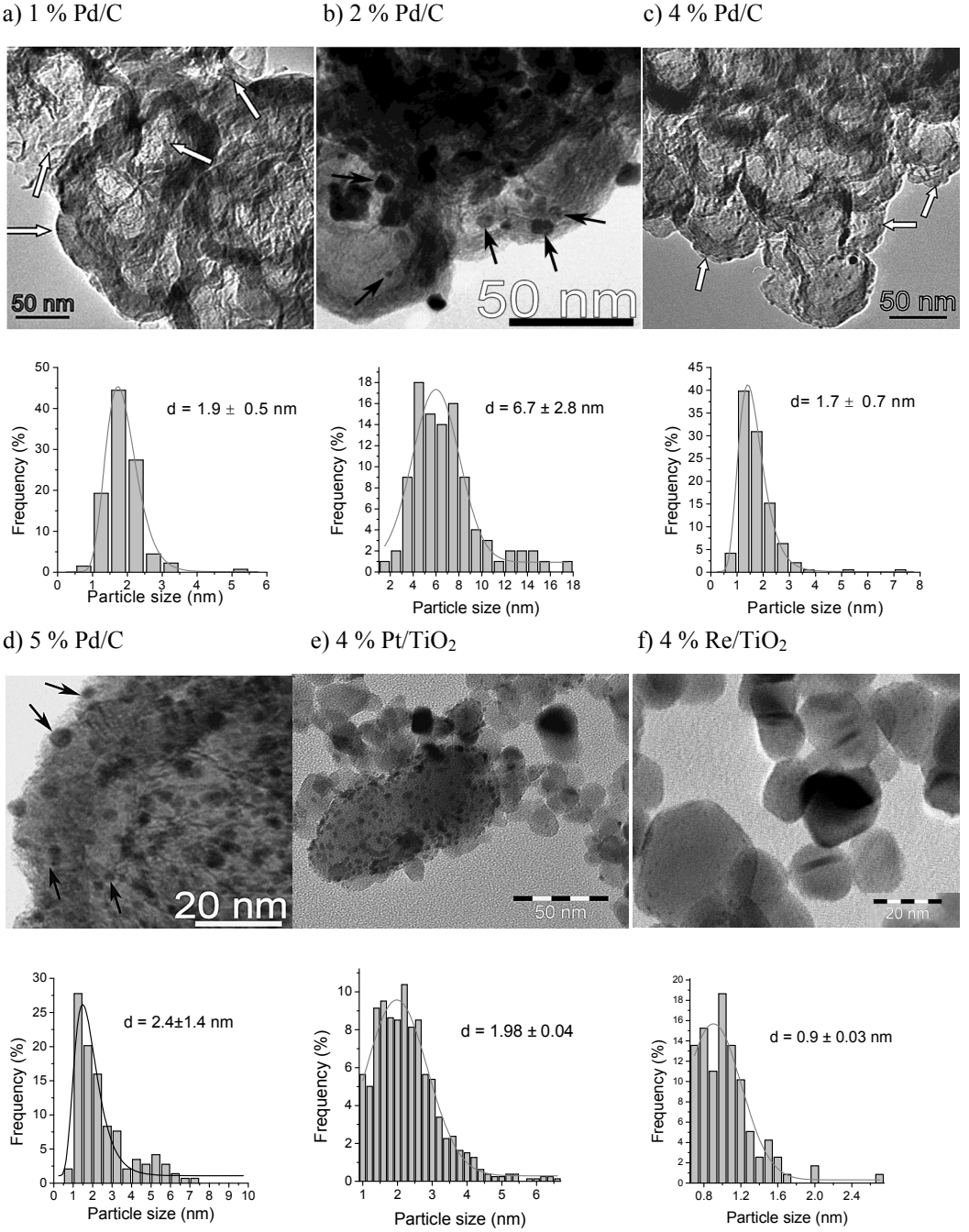

Figure 6. TEM images and particle size distribution of the catalysts.

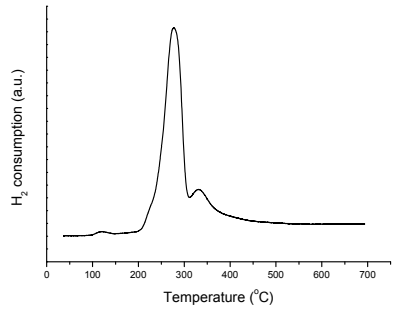

Figure 7. Temperature programmed reduction (TPR) of Re/TiO_2 catalyst.

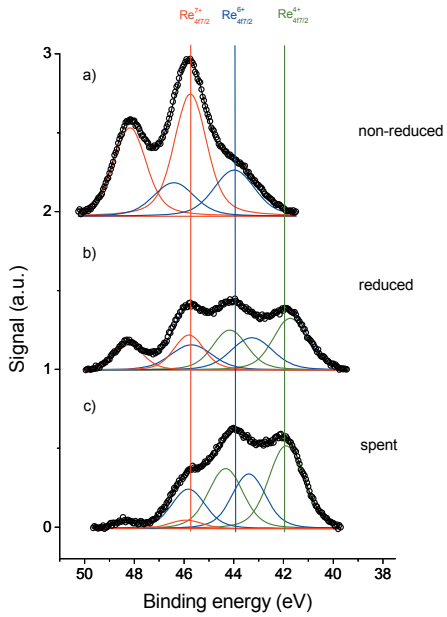

Figure 8. XPS rhenium species for: a) non-reduced catalyst; b) reduced catalyst at 400 °C for 2 h; c) spent catalyst after reaction with pre-reduced catalyst.

The dispersion varied from 26 % for 4 % Pt/TiO_2 to ~100 % for Re/TiO_2. In the case of Re/TiO_2, CO/metal ratio was 0.35. This low ratio is caused by only partial reduction of rhenium to Re^{4+} and Re^{6+}, and as the result, its lower affinity towards CO (*Table 2*).

The temperature programmed reduction was studied for the TiO_2–based catalysts. The reduction of 4 % Pt/TiO_2 and bimetallic 4 % Pt – 4 % Re/TiO_2 catalysts occurs at a low temperature, while for the 4 % Re/TiO_2 catalyst, the hydrogen uptake occurred at temperatures around 300 °C (*Figure 7*). Despite no hydrogen uptake after 450 °C, rhenium did not undergo complete reduction.

The XPS analysis revealed that the Re/TiO_2 catalyst after the reduction at 400 °C for 2 h was in a state of mixed oxide of Re^{4+}, Re^{6+} and Re^{7+} (*Figure 8*). However, the catalyst investigated after the reaction contained only Re^{4+} and Re^{6+}, indicating that the catalyst reduction was performed during the experiment **[VIII]**. Moreover, it should be mentioned that the oxidation of rhenium species can occur at room temperature being more profound with a decrease of nanoparticle size[43]. Therefore, it is difficult to estimate the exact amount of Re^{7+} in the reduced and spent catalysts, as the catalyst had a short contact with air during the transportation to the XPS instrument.

The acidity and basicity for the Pt, Re and PtRe catalysts were analyzed by temperature programmed desorption of NH_3 and CO_2, respectively. The results reveal an increase of the acidity and basicity of the catalysts after the metal deposition in comparison to bare TiO_2

(*Table 3*). A higher ammonia uptake was obtained with 4 % Pt/TiO_2 compared to 4 % Re/TiO_2 catalyst. The platinum catalyst had one desorption peak at 190 °C, whereas rhenium catalyst had two desorption maxima at 170 °C and 370 °C. Interestingly, for a bimetallic catalyst consist of platinum and rhenium, the ammonia uptake was the lowest despite a higher weight percentage metal loading.

Table 3. Acidity and basicity of TiO_2 supported catalysts.

	TPD	
	NH_3	CO_2
Catalysts	µmol/g	µmol/g
4 % Pt/TiO_2	322	253
4 % Re/TiO_2	270	531
4 % Pt – 4 % Re/TiO_2	254	386
TiO_2	15	37

Contrary to the acidity measurements, basicity of the catalyst was higher for rhenium catalyst in comparison with platinum catalyst, with the bimetallic catalyst being in the middle (*Table 3*). Platinum catalyst exhibited three desorption peaks at 80 °C, 240 °C and 380 °C, whereas the maxima for rhenium were at 80 °C, 160 °C and 350 °C.

3.2 Decarboxylation/decarbonylation of fatty acids over Pd/C

The catalyst chosen for studies of decarboxylation and decarbonylation was Pd/C, which was found to be the most active and selective catalyst in decarboxylation of fatty acids in the previous research[27,44]. Palladium nanoparticles were deposited over the Sibunit carbon support[45]. This mesoporous synthetic material is thermally more stable and mechanically resistant, which gives it an advantage over traditional activated carbon. Moreover, the mesoporous character of the material is suitable for a reaction with high molecular weight molecules.

3.2.1 Decarboxylation and decarbonylation of saturated fatty acids

Deoxygenation of lauric acid was performed over 5 wt% Pd/C at 300 °C and 2 MPa of total pressure **[II].** For understanding the reaction mechanism and role of the hydrogen in catalytic deoxygenation of fatty acids, inert and hydrogen–rich atmospheres were used in the experiments (*Figure 9*). The main reaction product was undecane, which was obtained by decarboxylation/decarbonylation of lauric acid. The yield of hydrocarbons was higher in hydrogen–rich atmosphere (TOF = 0.07 1/s [$mol_{substrate}/mol_{Pd\text{-}surface}/s$]), compared to the experiment in inert atmosphere where the initial deoxygenation rate was higher during the first 50 min (TOF = 0.12 1/s, calculated for 0–50 min), but its activity decreased with time keeping stable rate after 100 min (TOF = 0.045 1/s, calculated for 100–300 min) (*Figure 9b*). Moreover, formation of the undecane was suppressed in hydrogen–rich conditions.

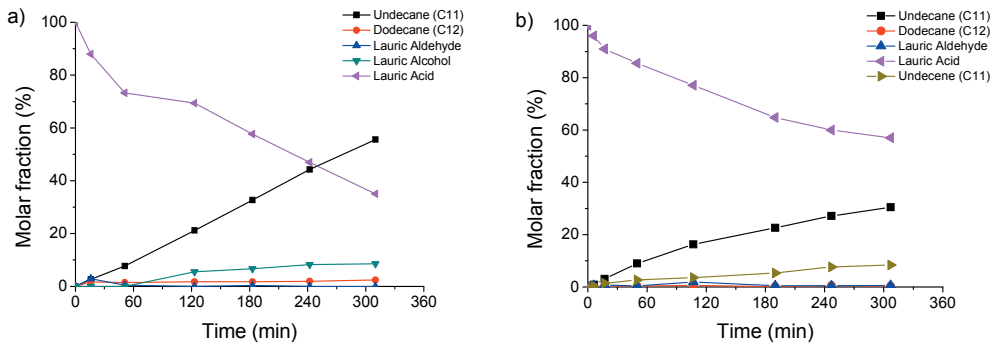

Figure 9. Transformation of 0.05 M lauric acid in hexadecane under: a) hydrogen; b) argon over 0.1 g of 5 % Pd/C catalyst, at 300 °C and 2 MPa of total pressure.

The selectivity towards the desired aliphatic hydrocarbons in the reaction with inert and hydrogen–rich atmosphere exceeded in both cases 90 % (*Figure 10*). However, in the hydrogen–rich atmosphere, the selectivity increased with increasing reactant conversion, which can be explained by the high formation of reaction intermediates which were gradually converted into products. Moreover, in the reaction under argon, traces of aromatic compounds were found in the mixture which is in line with the results reported previously **[III-V]**.

The gas–phase analysis during the lauric acid transformation revealed different reaction pathways, depending on the hydrogen content in the reaction medium. Previous studies have demonstrated, that in the absence of hydrogen, fatty acids deoxygenate predominantly via decarboxylation generating CO_2[27]. Transformation in the presence of hydrogen, however, proceeds through decarbonylation which generates CO as a main gas product.

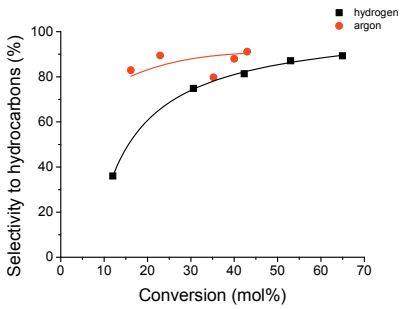

Figure 10. Selectivity vs. conversion in the reaction of 0.05 M lauric acid in hexadecane over 0.1 g of 5% Pd/C catalyst, at 300°C and 2 MPa of hydrogen or argon total pressure.

When hydrogen is present, the main products of lauric acid transformation are saturated hydrocarbons, predominantly undecane, which is a product of lauric acid decarbonylation, and dodecane which is a product of carboxylic group reduction. The yield of dodecane reached 2.5 % at the lauric acid conversion level of 65 %, which indicates that decarboxylation/decarbonylation is predominant in comparison with carboxylic group reduction at 300 °C over 1 % Pd/C catalyst.

In experiments performed in the absence of hydrogen in the reaction system, as expected, no dodecane was noticed. Moreover, in contrast to the experiments in the hydrogen–rich atmosphere, significant yields of unsaturated hydrocarbons were observed.

Lauryl alcohol was observed in the reaction mixture under the hydrogen–rich atmosphere. Its presence was expected as it is an intermediate of the carboxylic group hydrogenation, however, only traces of lauric aldehyde were observed. To understand the conversion pathways of the intermediates experiments with inert and hydrogen–rich atmosphere were performed.

3.2.1.1 Deoxygenation of reaction intermediates

The experiments with the reaction intermediates lauryl alcohol and lauric aldehyde were performed under the same conditions as the experiments with lauric acid to understand in more depth the reaction pathway over Pd/C catalyst **[II]**.

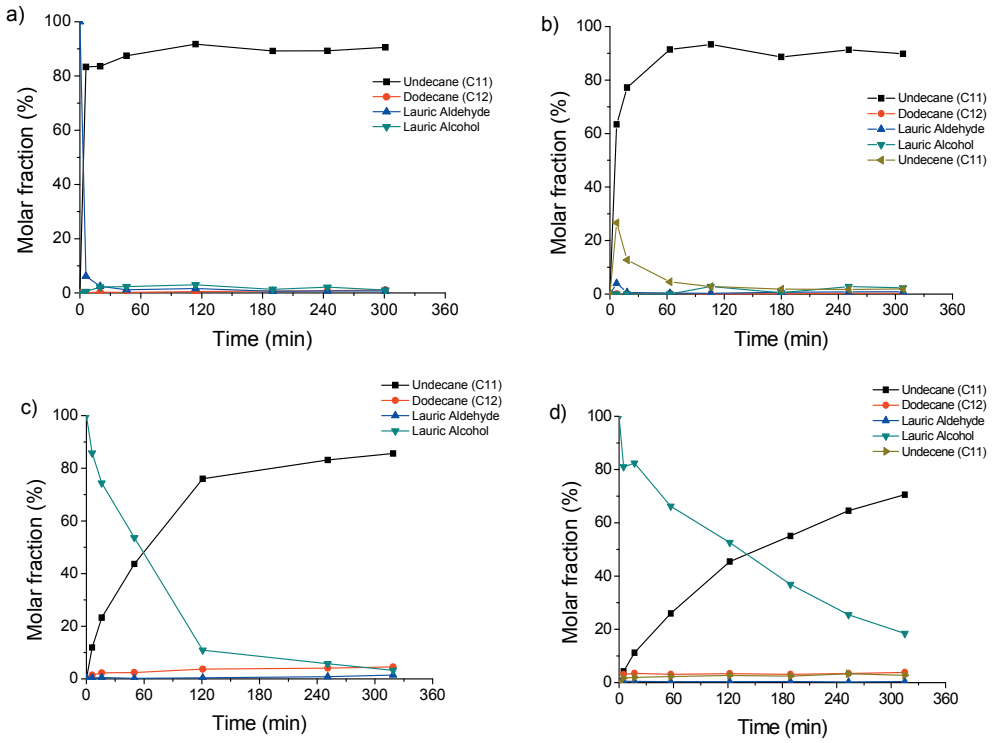

Figure 11. Transformation of 0.05 M lauric aldehyde (a, b) and lauryl alcohol (c, d) in hexadecane under: hydrogen (a, c) and argon (b, d) over 0.1 g of 5 % Pd/C catalyst, at 300 °C and 2 MPa of total pressure.

The experiments revealed that decomposition of lauric aldehyde was almost instantaneous leading to a complete conversion of lauric aldehyde to hydrocarbons during the first 5 minutes, both in Ar and H_2 atmospheres (*Figure 11a, b*). The main product was undecane, which indicates that the transformation of aldehyde was highly selective towards decarbonylation. The hydrogenation of lauric aldehyde was minor leading to the formation of traces of dodecane. In the inert atmosphere unsaturated products (undecene) were formed with the yield reaching 26 % at total conversion. Gradually, these products were hydrogenated to undecane, as hydrogen was

generated from dehydroformylation of lauric aldehyde to undecene and from dehydrogenation of the solvent (hexadecane), which was observed as well in the blank experiment.

The decomposition of aldehydes over the palladium surface is a well-known reaction which occurs over Group VIII metals, such as Rh, Pt or Pd [46,47]. Due to the high rate of the aldehyde decomposition only traces of aldehyde can be detected with chromatographic methods. This explains the presence of only traces of lauric aldehyde in the reaction mixture during the transformation of fatty acids, with simultaneously significant amounts of lauryl alcohol, which is an intermediate in the reduction of lauric acid.

The conversion of lauryl alcohol, after 300 min of reaction, reached 98 % and 81 % in H_2 and Ar atmosphere, respectively. The main reaction product was undecane with a selectivity exceeding 85 % for both gas atmospheres at the end of the reaction (*Figure 11c, d*). Some dodecane formation was observed in both experiments, with slightly higher amounts under the hydrogen–rich atmosphere.

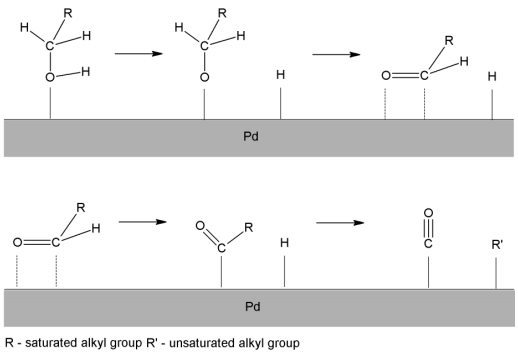

Figure 12. Mechanism of alcohol decomposition over Pd(111). Adapted from ref. [48].

The formation of undecane suggests that a further hydrodeoxygenation of the alcohol to dodecane is not a favorable reaction step. The conversion of lauryl alcohol to undecane proceeds through dehydrogenation to the aldehyde surface species and thereafter, decarbonylation to hydrocarbons on the palladium surface (*Figure 12*) as it has been suggested in literature[48].

3.2.1.2 Fatty acids reaction pathway over Pd/C catalyst

It can be generally stated that hydrogen has a strong influence on the reaction pathways of fatty acids deoxygenation over Pd/C catalysts. Under an inert atmosphere, the hydrocarbon formation

occurs via decarboxylation of fatty acids with CO_2 as the predominant gaseous product[27,49]. However, deoxygenation of fatty acids under hydrogen–rich conditions has a more complex reaction pathway. As the palladium surface is highly saturated with hydrogen, hydrogenation of carboxylic group occurs. The aldehyde formed decomposes through decarbonylation producing CO **[II]**. Alcohol which is formed during the reaction undergoes dehydration to form an aldehyde which decomposes to undecane. Dodecane, which is the product of the alcohol hydrogenation, was formed with the highest yield in the experiment with alcohol under hydrogen atmosphere, however, its content reached only 4.5 mol% at a 97 mol% conversion level. Therefore, it can be stated that total hydrogenation of carboxylic group over Pd/C catalyst is not a favorable reaction. The overall reaction network is illustrated in *Figure 13*.

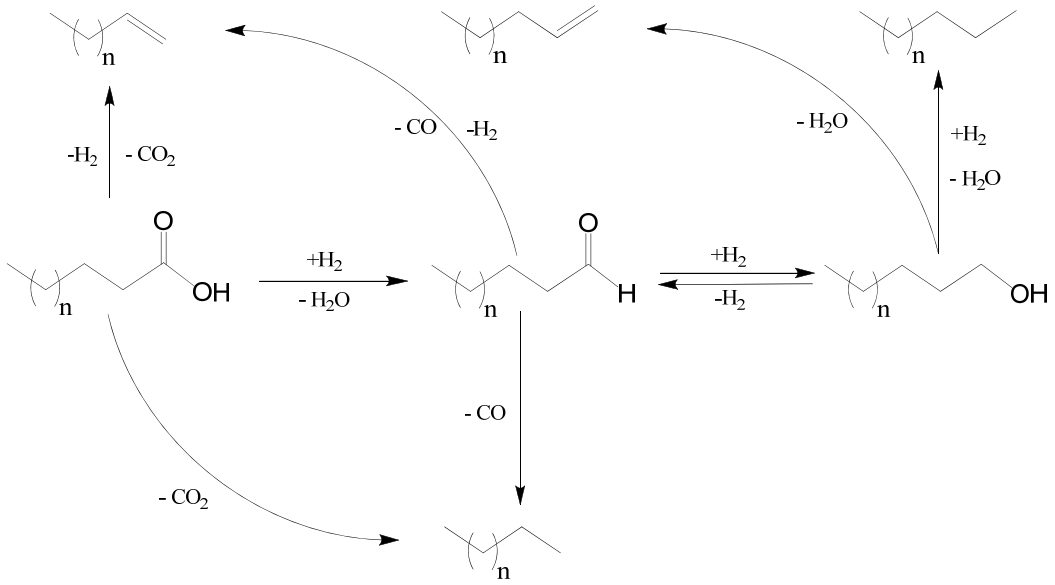

Figure 13. Lauric acid deoxygenation pathways over Pd/C catalyst.

3.2.2 Deoxygenation of unsaturated fatty acids

Deoxygenation of unsaturated fatty acids was performed with unsaturated model compounds and industrially available feedstock over 1 % Pd/C with 1 % hydrogen in argon at 1.7 MPa of total pressure. The model compounds chosen for this reaction were oleic and linoleic acids **[III]**, whereas, tall oil fatty acids (TOFA) **[IV, V]** were selected as an example of industrial feedstock available in Finland.

The deoxygenation was performed at 300 °C for fatty acids diluted in dodecane at initial concentration of 0.15 M. To mimic different unsaturation levels of fatty acids, (9*Z*)-9-octadecenoic (oleic) and (9*Z*,12*Z*)-octadeca-9,12-dienoic (linoleic) acids were chosen with one and two double bonds, respectively, and the fully saturated stearic acid as a comparison.

The conversion of fatty acids increased with decreasing unsaturation in the order stearic acid>oleic acid>linoleic acid (*Figure 14a*). Stearic and oleic acid initial reaction rates were the same, while the linoleic acid conversion was significantly lower. With increasing time the rate of oleic acid transformation decreased, indicating, catalyst deactivation.

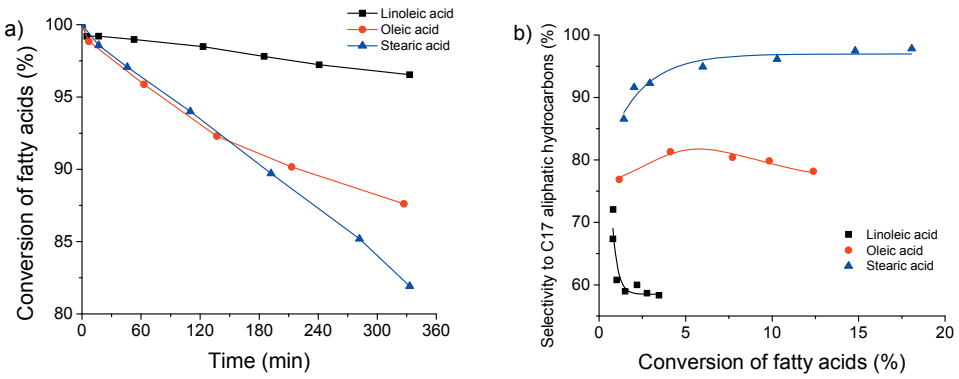

Figure 14. a) Conversion; b) selectivity towards aliphatic hydrocarbons – in reaction with of 0.15 M stearic, oleic and linoleic acid in dodecane at 300 °C and 1.7 MPa (1 % H_2 + Ar) of total pressure.

As unsaturated fatty acid is injected to the reactor it undergoes *cis-trans* isomerization and further hydrogenation of the double bond and simultaneous decarboxylation/decarbonylation yielding C_{17} saturated and unsaturated hydrocarbons. Moreover, aromatic compounds (e.g. undecylbenzene) were detected as cyclization products of fatty acids and further dehydrogenation of the ring due to the hydrogen deficiency in the system. Furthermore, heavy

by–products were detected in forms of oligomers by size-exclusion chromatography with an increasing content with fatty acids unsaturation. The above mentioned by–products were not formed or appeared only to a small extent in the experiments with stearic acid.

The selectivity towards linear hydrocarbons increased with a decreasing unsaturation of fatty acid (*Figure 14b*). In the reaction with stearic acid, 98 % of fatty acid was converted to aliphatic hydrocarbons, while in the case of oleic and linoleic acids the selectivity was around 80 % and 60 %, respectively. The main reason of the decreased selectivity to linear hydrocarbons was the formation of aromatic species. The reaction pathway for unsaturated linoleic and oleic acid over 1 % Pd/C catalyst is displayed in *Figure 15*.

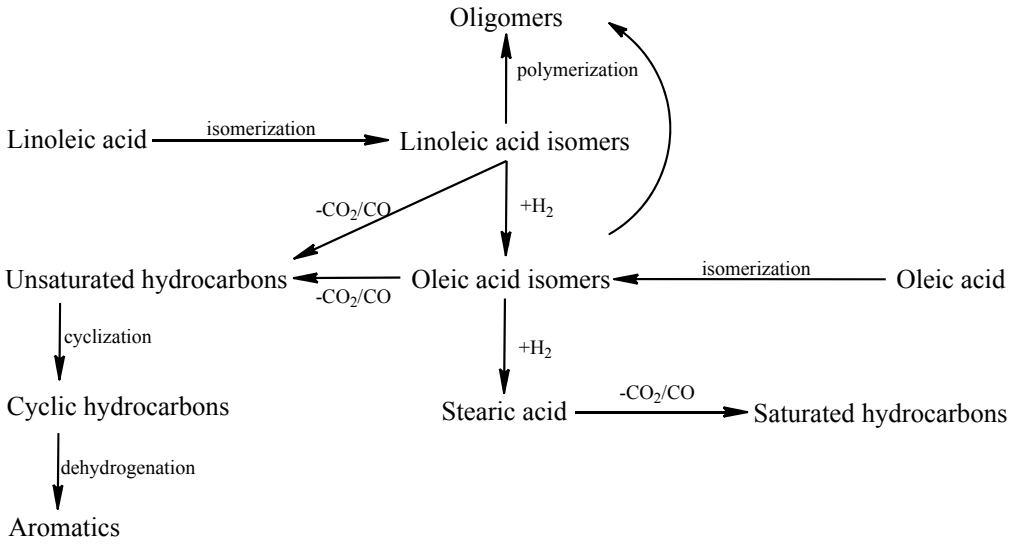

Figure 15. Reaction pathway in the deoxygenation of linoleic and oleic acids on 1 % Pd/C catalyst.

3.2.3 Deoxygenation of tall oil fatty acids

Tall oil fatty acids (TOFA) are industrially available feedstock originated from wood. It contains 97 % of fatty acids from which unsaturated linoleic and oleic acids are the predominant compounds.

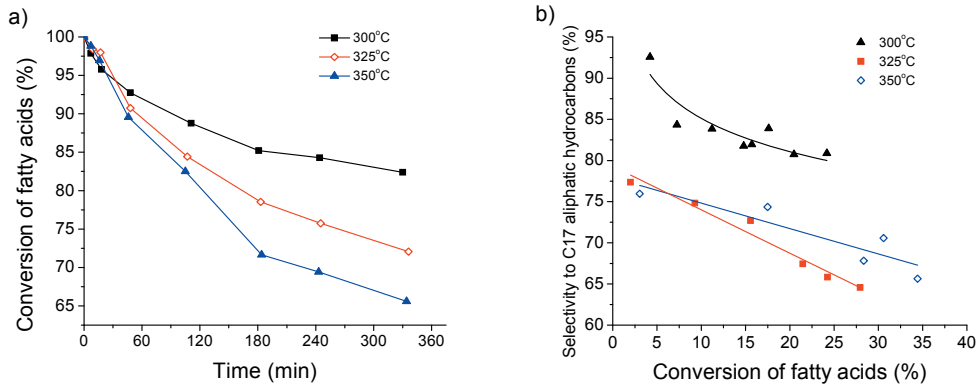

Figure 16. Conversion of TOFA and selectivity to C17 aliphatic hydrocarbons at 1.7 MPa (1 %H_2+Ar), c_0 = 0.15 M.

Deoxygenation of TOFA was performed at 300–350 °C in 1 % H_2 in Ar at the total pressure of 1.7 MPa **[IV, V]**. Similarly to experiments with model compounds (*Section 3.2.2*), unsaturated fatty acids went through isomerization at the beginning of the reaction. Thereafter, the isomers were hydrogenated partially to stearic acid. The main products were aliphatic C_{17} hydrocarbons while the main by–products were C_{17} aromatic compounds.

As expected, the increase of the reaction temperature increased the conversion of fatty acids. However, the selectivity to aliphatic hydrocarbons decreased for reactions above 300 °C (*Figure 16*). Moreover, the selectivity decreased with an increase of the conversion in reactions between 300–350 °C in 1 % of H_2 in Ar atmosphere, indicating a higher selectivity towards aromatic species as the reaction proceeds, especially at higher temperatures.

Hydrogenation of the double bonds in the fatty acids was higher at lower temperatures. Moreover, with an increase of reaction temperature more unsaturated hydrocarbons were formed. This can be a result of a more profound thermodynamically favored dehydrogenation at higher temperatures as well as a decrease of available hydrogen on the palladium surface. These are

manifested in higher levels of unsaturated fatty acids and formation of unsaturated hydrocarbons, which were transformed further to aromatic species.

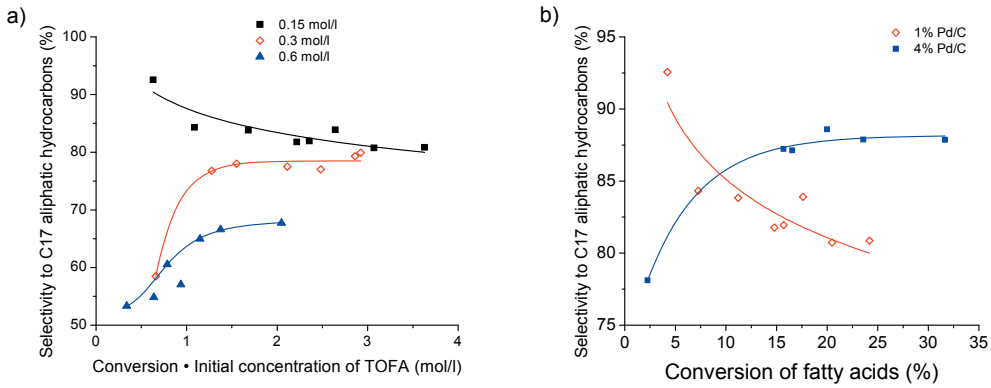

Figure 17. Selectivity to aliphatic hydrocarbons vs. conversion of fatty acids: a) at different initial concentration of TOFA (0.15–0.6 M); b) at different palladium loading (1 % and 4 %) in deoxygenation of TOFA over 0.5 g Pd/C (Sibunit) catalyst at 300 °C and 1.7 MPa (1 % H_2 + Ar).

A similar effect was observed in experiments with higher concentrations of TOFA (0.15–0.6 M). With initial concentrations of 0.3 M and 0.6 M of TOFA hydrogenation of unsaturated fatty acids to stearic acid reached 17 % and 5 % after 330 min of reaction, respectively. In comparison at the TOFA concentration of 0.15 M, the yield of stearic acid was 57 %. An increase of the ratio between the fatty acids and palladium led to a lower hydrogenation of fatty acid double bonds, and therefore, a higher formation of aromatic compounds and a lower selectivity to linear hydrocarbons (*Figure 17a*).

The opposite effect was observed in the reactions with the 4 % Pd/C catalyst. An increase of the ratio between active sites and unsaturated fatty acids led to increased hydrogenation to stearic acid, and therefore, a lower formation of byproducts (*Figure 17b*).

3.2.3.1 Deoxygenation of TOFA under hydrogen–rich atmosphere

For the sake of comparison with the experiment in 1 % H_2 atmosphere, experiments in hydrogen atmosphere were performed at 300 °C and 350 °C. The initial conversion rate of fatty acids was the same in comparison to the experiment at 1 % H_2. In the 1 % H_2 atmosphere, the catalyst deactivation occurred while in the hydrogen–rich atmosphere, the conversion rate remains constant. It was especially visible in reactions at 350 °C (*Figure 18a*).

The selectivity towards aliphatic hydrocarbons for reactions at 350 °C increased considerably from ~70 % in the reaction with 1 % H_2 to 90 % in pure H_2. Moreover, the selectivity was stable at the same level from 10–60 % conversion, which indicates a good stability of the catalyst even at high temperatures (*Figure 18b*). The lower selectivity at lower conversion levels for reactions at 350 °C in hydrogen was caused by the low saturation of palladium surface by hydrogen at the beginning of the reaction.

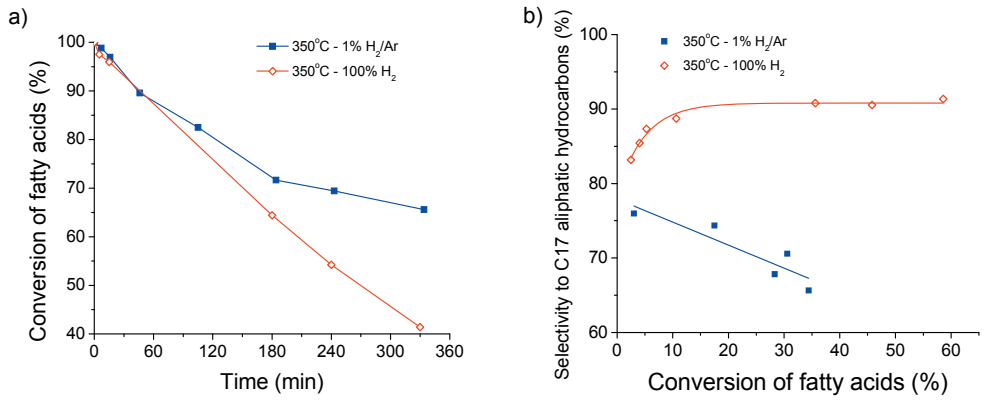

Figure 18. Deoxygenation of 0.15 M TOFA diluted in dodecane over 0.5g of 1 % Pd/C catalyst at 350 °C and 1.7 MPa and different hydrogen content: a) conversion of fatty acids; b) selectivity to aliphatic hydrocarbons vs. conversion of fatty acids.

Deoxygenation in hydrogen at lower temperatures leads to a further increase of the selectivity to linear hydrocarbons. The selectivity obtained at 300 °C was already 94 % at 20 % conversion (*Figure 19a*). Moreover, the level of aromatic compounds after the initial formation (0.8 % at conversion 0–7 %) increased only by 0.5 % at the conversion level between 7–27 %.

The experiments under a pure hydrogen atmosphere and effects observed with experiments at different temperatures and initial concentrations suggest that the hydrogenation of double bonds is crucial for a high selectivity and a good stability of the catalyst. The hydrogenation of double bonds can be achieved either during the reaction, or alternatively, the other option is a two–step process where pre–hydrogenation of unsaturated fatty acids to its saturated form can be achieved efficiently at lower temperature. Thereafter, a subsequent deoxygenation of saturated fatty acids can be performed at higher temperatures over the same catalyst (*Figure 19a*).

The 0.15 M TOFA solution was hydrogenated over 1 % Pd/C at 120 °C for 80 min (*Figure 19b*) and the main reaction product was stearic acid. Thereafter, the temperature was raised to 300 °C and the deoxygenation reaction was performed under 1% H_2 in Ar.

The selectivity towards linear hydrocarbons after pre–hydrogenation of TOFA was stable at the level of 95 %. In comparison to the experiments performed under pure hydrogen, both yields of the desired products and by–products as well as the conversion levels were similar, indicating the feasibility of the pre–hydrogenation method.

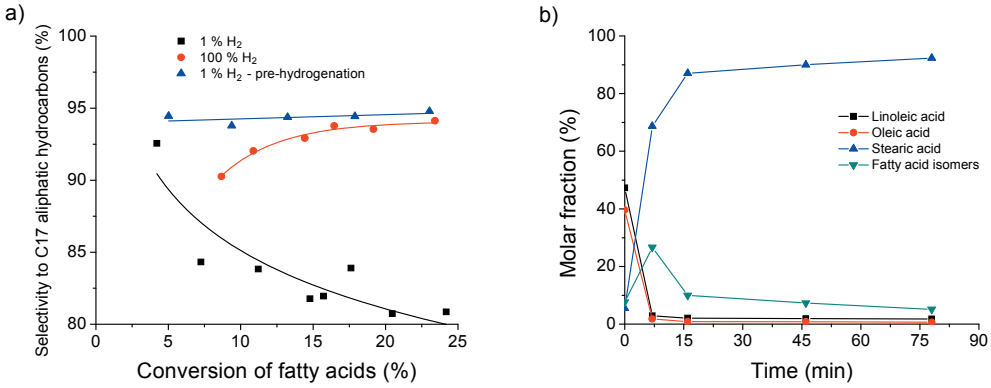

Figure 19. a) Selectivity to aliphatic hydrocarbons vs. conversion of fatty acids in deoxygenation of 0.15 M TOFA diluted in dodecane over 0.5 g of 1 % Pd/C catalyst at 300 °C and 1.7 MPa – effect of pre–hydrogenation of TOFA; b) hydrogenation of 0.15 M TOFA in 1 % H_2/Ar at 120 °C and 1.7 MPa.

3.2.4 Deoxygenation in fixed bed reactor

Previous studies contributed to the understanding of the reaction pathways. Model compounds over Pd/C catalyst were used and their activity and selectivity were predicted. Furthermore, the studies with TOFA, deepened the knowledge about the utilization of industrially available feedstock and determined the challenges connected with it. However, to fully understand the catalyst behavior, long lasting stability experiments were carried out. The egg–shell 2 % Pd/C the catalyst in a fixed bed reactor was used for deoxygenation of stearic acid **[VI, VII]**, ethyl stearate **[VII]** and technical tristearin **[VII]** at 300 °C and 2 MPa of total pressure. The experiments were conducted in pure argon and 5 % H_2/Ar to determine the response of the catalyst for step changes of the gas phases. Moreover, catalyst deactivation profile through the reactor for molecules with various functional groups in the C_{18} fatty feedstock was studied.

3.2.3.1 Step changes behavior for diluted stearic acid

Stearic acid (10 mol%) diluted in dodecane was converted over 10 g of 2 % Pd/C catalyst (*Figure 20*) **[VI]**. An inert atmosphere was used at the beginning of the reaction **(I)**. The main gaseous product was CO_2 indicating that the reaction proceeded mainly through decarboxylation of stearic acid. Thereafter, a step change to 5 % H_2/Ar was performed at TOS = 300 min. The yield of the main product heptadecane rapidly increased and CO_2/CO ratio decreased to ~2 **(II)**. The catalyst was stable under these conditions with no indication of any deactivation for over 1000 min time–on–stream (TOS). Subsequently, pure argon was introduced to the system **(III, IV)** and the experiment was continued for another 1500 min. After the step change to argon, heptadecane yield dropped by 25 %. Moreover, the formation of CO decreased and CO_2 once again was the main gas product of the reaction. However, with time the CO formation increased gradually until the TOS = 2650 where the formation of CO started to increase rapidly, which was followed by a rapid drop of the CO_2 formation almost to zero. Moreover, the yield of heptadecane declined rapidly indicating a sudden deactivation of the catalyst. Thereafter, the feed was substituted to dodecane and the reaction stopped **(V)**.

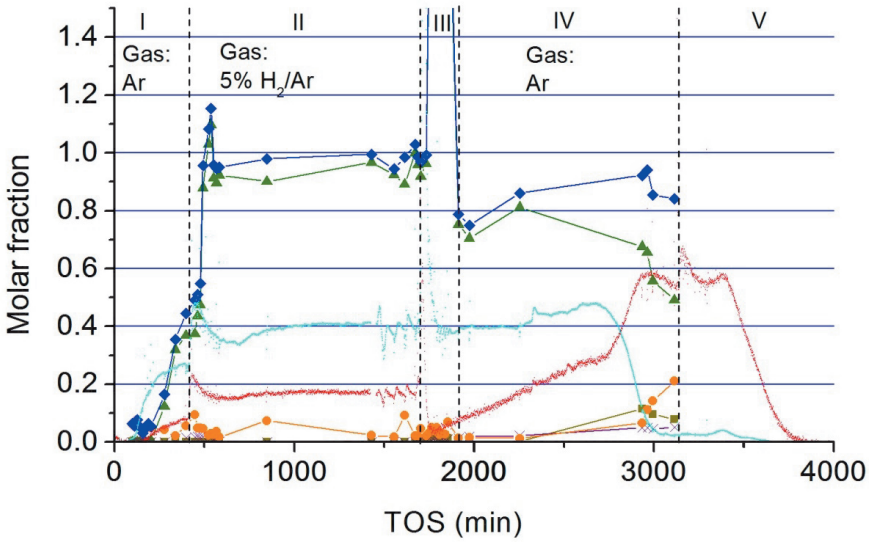

Figure 20. Decarboxylation in liquid flow of stearic acid over Pd/C at 300 °C diluted in dodecane at 0.075 ml/min, 5 % H_2/Ar, or pure Ar gas at 20 bar at 42 ml/min. Changes in the operating parameters: (I) gas = Ar, (II) gas = 5 % H_2/Ar, (III) erroneous liquid sampling, (IV) gas = Ar, (V) liquid = dodecane. Legend: Liquid mole balance (dark blue diamonds), stearic acid (orange circles), heptadecane (green triangles), heptadecene (dark yellow squares), undecylbenzene (purple ×), CO (red dots), CO_2 (light blue dots).

The experiments confirmed that a stable transformation of diluted stearic acid can be achieved in a 5 % H_2/Ar atmosphere during a prolonged experiment. Catalyst deactivation occurred under the inert atmosphere. The reason of a shift in gas selectivity from CO_2 to CO is unclear, but it can be observed that the catalyst deactivation is in line with the accumulation of CO in the system. During the experiment with an inert gas atmosphere, formation of aromatic compounds was observed, which could cause catalyst deactivation. Moreover, carbon monoxide can poison the catalyst surface since there is no significant amount of hydrogen to clean the palladium surface.
Formation of CO required hydrogen present on the surface of the catalyst. During the experiment under an inert atmosphere, an increased yield of unsaturated hydrocarbons was noticed, which could explain the CO formation under hydrogen deficient conditions.

3.2.3.2 Deoxygenation of neat stearic acid, ethyl stearate and technical tristearin

Some model compounds were selected to mimic the deoxygenation of a feed containing different functional groups **[VII]**. Solvent–free experiments were performed at 300 °C and 2 MPa of total pressure. Each of the experiment was conducted under a 5 % H_2/Ar atmosphere for 4500–5500 min. Thereafter, the gas was switched to argon and the reaction was continued to TOS ~9000 min. In all of the reactions, the main products were n-1 (carbon number) hydrocarbons indicating no changes in selectivity within the liquid–phase hydrocarbon products with a change of the feed.
At the beginning of the experiment with neat stearic acid, the selectivity in both gas and liquid phases was similar to the results obtained with diluted stearic acid (Section 3.2.3.1). However, in experiments with concentrated acid the heptadecane yield decreased slightly over time (*Figure 21a*). Moreover, the CO formation increased gradually with a decrease of CO_2 in the gas phase. The formation of CO was consistent with the increase of the hydrogen consumption (*Figure 22a*). No light hydrocarbons were detected, which indicates that neither cracking nor methanation of CO_x take place during the deoxygenation.
As 5 % H_2/Ar was substituted with an inert gas at TOS = 5760 min, the yield of hydrocarbons suddenly dropped. The catalyst was deactivated which can be visible as the CO_2 formation after an initial rapid increase dropped to zero (*Figure 21a*). A similar behavior was observed for reactions with ethyl stearate and technical tristearin, where no formation of hydrocarbons products was observed after the switch to inert reaction atmosphere (*Figure 21b, c*).

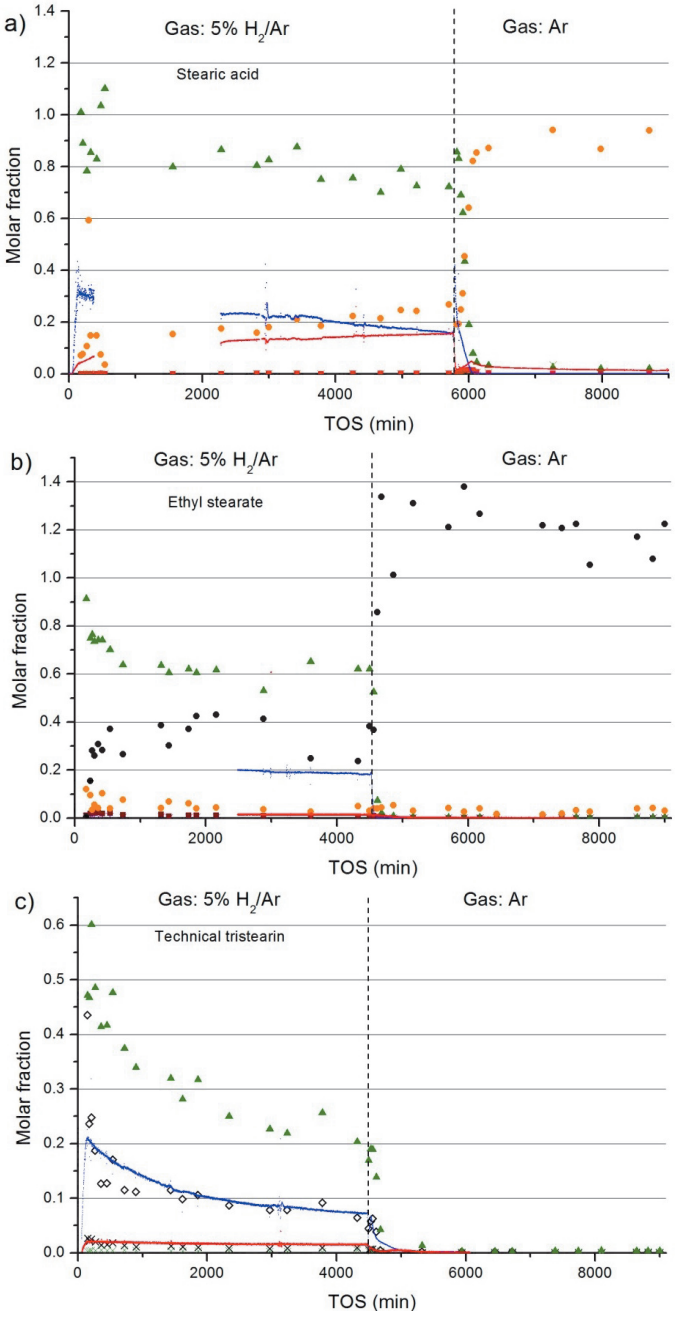

Figure 21. Reaction with: a) stearic acid; b) ethyl stearate; c) tristearin over 2 % Pd/C at 300 °C and 2 MPa of total pressure. Symbols: (*red filled square*) 1–heptadecene, (*green filled triangle*) heptadecane, (*purple x*) aromatics, (*orange filled circles*) stearic acid, (*black filled circles*) ethyl stearate, (*black filled diamond*) pentadecane, (*black x*) hexadecane, (*green x*) octadecane, (*red line*) CO, (*blue line*) CO_2.

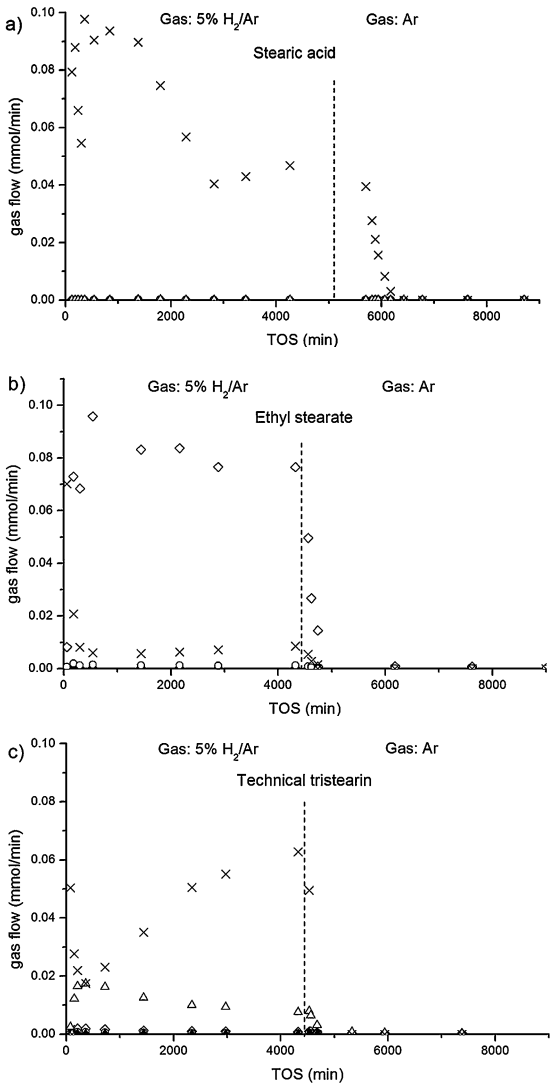

Figure 22. Molar flows of gas-phase products during deoxygenation of stearic acid, ethyl stearate and tristearin. Symbols: (x) H_2, (circle) methane, (open diamond) ethane and (spade) propane

The conversion of ethyl stearate after an initial decrease was stable over time in the 5 % H_2/Ar atmosphere (*Figure 21b*). However, a significant deactivation of the catalyst was observed for technical tristearin with a conversion decline exceeding 60 % within 4500 min on stream (*Figure 21c*).

The gas–phase analysis revealed the formation of light hydrocarbons: ethane in the reaction with ethyl stearate and propane in the reaction with tristearin (*Figure 22b, c*) which were formed after the deoxygenation of the corresponding esters. No other light hydrocarbons were detected, indicating that no cracking occurred.

The hydrogen consumption in the reaction with ethyl stearate and tristearin was high, since it is needed to break the ester bond. In the experiment with ethyl stearate, the hydrogen consumption remained at a high level through the whole reaction period, while in the experiment with tristearin it decreased with time as the catalyst deactivation proceeded (*Figure 22b, c*).

Interestingly, in the experiments with ethyl stearate and tristearin, the formation of CO was minor compare to the conversion of neat stearic acid. These phenomena could indicate a different reaction mechanism of ester deoxygenation as only a small quantity of stearic acid was found in the liquid phase in both ethyl stearate and tristearin reactions.

3.2.3.3 Deactivation of Pd/C catalyst during long lasting deoxygenation in fixed bed reactor

Nitrogen physisorption measurements were performed for the spent catalysts to determine a possible decrease of the catalyst specific surface area. The catalyst bed was divided into 5 or 6 parts separated with glass wool for easy extraction (*Figure 23a*). Thereafter, the catalyst was washed with hot ethanol and dried afterwards before the measurements.

In the experiments with diluted stearic acid the surface area decreased by 72 % at the beginning of the bed. The decrease in the surface area and the total pore volume was higher at the inlet of the bed and decreased along with the height of the reactor **[VI]**.

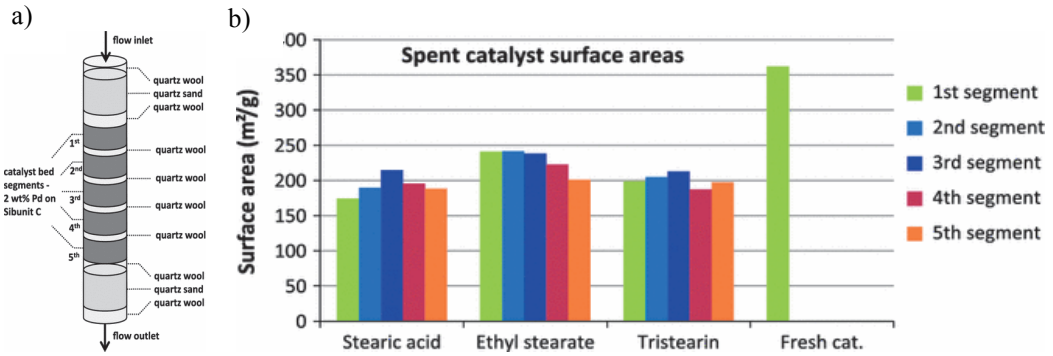

Figure 23. Suface area decrease in deoxygenation of stearic acid, ethyl stearate and tristearin: a) a schematic picture of the trickle bed reactor loaded with catalyst in five separated segments; b) the specific surface areas of the fresh and spent catalysts for each of the deoxygenation substrates as a function of segment no. from the top in the catalyst bed

The decrease in the surface area was observed as well in the experiments with a neat feedstock **[VII]**. The average surface area decreased by 46 %, 36 % and 44 % for experiments with neat stearic acid, ethyl stearate and tristearin, respectively. The smallest decrease of the surface area for the experiment with ethyl stearate is in agreement with the highest stability of the catalyst during that reaction. However, the spent catalyst profile of the surface area is inconsistent with previous experiments with diluted stearic acid. In the reaction with neat stearic acid, the surface area was lowest at the reactor inlet and increased along the reactor length. However, at the reactor outlet, the surface area decreased again (*Figure 23b*). This inconsistency is caused probably by the heat distribution along the reactor bed: the heater was built up from aluminum blocks with the heat source connected at the bottom and a thermocouple was placed in the middle of the bed. Moreover, when focusing on the first three segments of the catalyst bed, it can be observed that

the highest gradient of the surface area was observed in the experiment with neat stearic acid in comparison to experiments with ethyl stearate and tristearin (*Figure 23b*), which can indicate differences in the mechanisms with different fatty acid derivatives.

The decrease in specific surface area was caused probably by coking of the catalyst, which was confirmed by a decrease in the pore volume and the percentage of mesopores and with an increasing percentage of micropores in the spent catalyst **[VI]**. A similar effect was observed in deoxygenation of TOFA with 1 % Pd/C **[V]**.

Leaching of the catalyst metal was found to be minor with 0.58 % of the total palladium content in the catalyst bed found in the post–reaction mixture of the experiments with diluted stearic acid **[VI]**. These results are in agreement with the literature[49,50].

An average particle size of the spent catalyst was marginally larger and no profound sintering was observed **[VI]** which is in line with the previous studies[41,49–51].

3.3 Deoxygenation over TiO_2 supported metal catalysts

The Pd/C catalyst proved to be active and selective in the deoxygenation of fats and free fatty acids. However, problems occurred with the formation of undesired species from unsaturated fatty acids or formation of carbon deposits on the surface of catalyst. Both of these effects can cause catalyst deactivation and are attributed to the elevated temperature of the process. Therefore, more active, new catalytic materials have to be found which will allow performing the reactions at lower temperatures.

The TiO_2 supported metal catalysts were active at 200 °C which allowed the negative effects attributed to high temperatures to be avoided. The unusually high activity of the catalysts is connected with the TiO_2 oxygen vacancies[35]. It was proposed that the fatty acid molecule bond on the interface of the metal nanoparticle with an α–carbon bond to the active metal and carbonyl oxygen to the Ti^{3+} surface species. This bonding weakens the C=O carbonyl bond and allows the proton from the metal surface to attack the α–carbon (*Figure 24*). A similar mechanism has been proposed for the synthesis of hydrocarbons over Ni/TiO_2 catalyst[30] or for synthesis of alcohols over $Ru–Sn/TiO_2$ and Pt/TiO_2 catalysts[35,36].

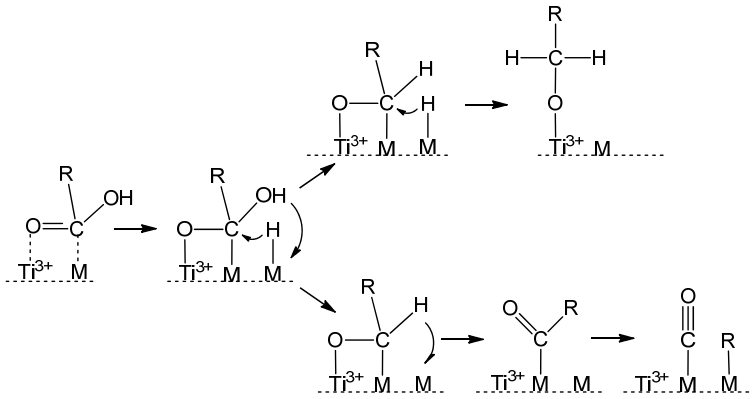

Figure 24. Mechanism of fatty acid deoxygenation over TiO_2 supported metal catalysts.

The experiments proved the different selectivities towards the desired product, depending on the active metal on the surface of TiO_2 (*Figure 25*). Pt/TiO_2 is selective towards hydrodeoxygenation to produce n–carbon alkanes, whereas over Ru/TiO_2 catalyst, the main reaction is decarboxylation/decarbonylation to n-1–carbon hydrocarbons. A special case is Re/TiO_2 which

shows a high selectivity to both alcohols and hydrocarbons depending on the residence time of fatty acids over the catalyst.

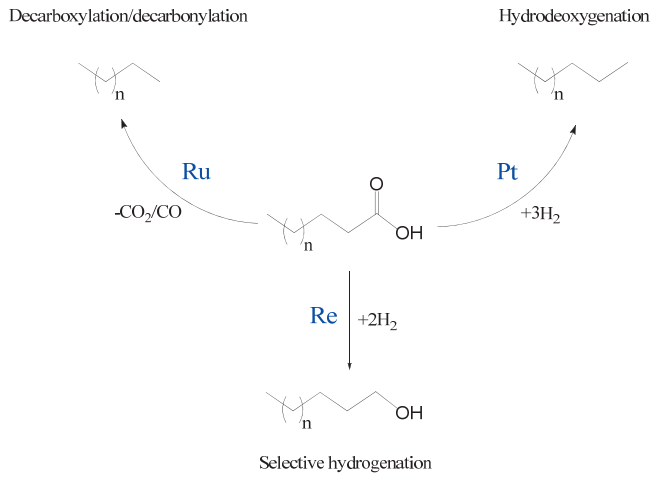

Figure 25. Simplified reaction pathways for TiO_2 supported metal catalysts

In addition, to the reaction pathway over the Pd/C catalysts (*Figure 13*), the formation of wax ester was observed. The stearyl stearate was formed from the reaction of fatty acid and fatty alcohol in reactions with Pt/TiO_2 at the highest experimental temperature (220 °C) and low pressure (2MPa) and in all reactions over the Re/TiO_2 catalyst.

3.3.1 Hydrodeoxygenation over Pt/TiO_2 catalyst

Experiments with Pt/TiO_2 were performed at 180–220 °C and 2–4 MPa. Conversion of fatty acids increased with a decrease of the reaction temperature and an increase of the hydrogen pressure (Figure 26a). Stearic acid was hydrogenated first to the corresponding alcohol and thereafter to octadecane. The formation of the (n-1)–carbon heptadecane occurred through the decarbonylation of an aldehyde surface species. However, the formation of heptadecane was minor and did not exceed 10 % at the end of the reaction in all the experiments (*Figure 26b*).

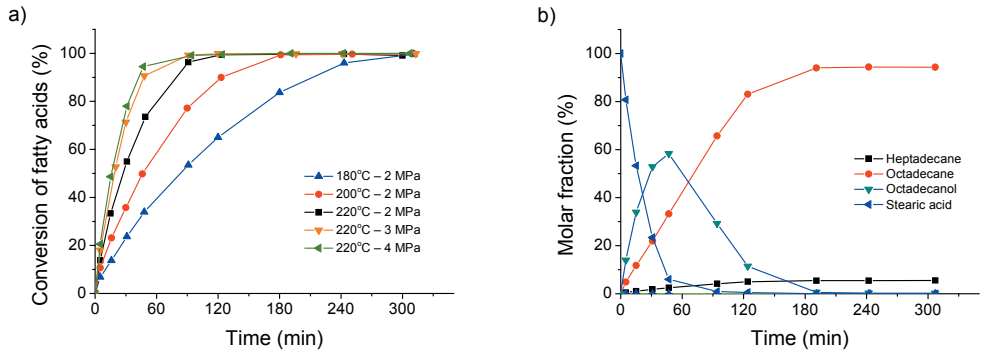

Figure 26. Hydrodeoxygenation of stearic acid over 4 % Pt/TiO_2 catalyst: a) conversion of fatty acids vs. time; b) reaction at 220 °C and 4 MPa of total pressure.

The decrease in the reaction temperature resulted as expected in a decrease of the stearic acid conversion, but an increase of the selectivity towards octadecane. The increase is significant as a decrease in the temperature by 40 °C from 220 °C to 180 °C resulted in a rise of the selectivity by 8 % at 25 % oxygenates conversion level (*Figure 27a*). Moreover, a higher selectivity to octadecane can be achieved by an increase of the hydrogen pressure. The increase by 2 MPa shifted the selectivity level at a full conversion of oxygenates by 4 % (*Figure 27b*).

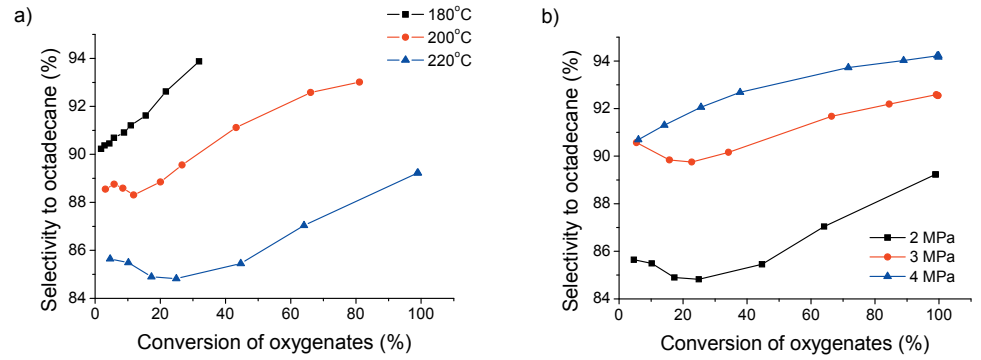

Figure 27. Selectivity to octadecane vs. conversion of oxygenates (stearic acid, octadecanol and stearyl stearate): a) temperature dependence at 2 MPa of total pressure; b) pressure dependence at 220 °C.

Such a high (94 %) selectivity in the hydrogenation of fatty acids to hydrocarbons with the same carbon number is the highest reported selectivity. In the literature it is reported that a 90 % selectivity has been achieved over sulfided Mo/Al_2O_3[21]. Moreover, the conversion at 180 °C

reached 30 % with a selectivity 94 %, which was still increasing. Therefore, the final selectivity could be even higher. Furthermore, the use of a high pressure at a low temperature should increase both the reaction rate and the selectivity to octadecane.

An initial drop of selectivity at low conversion levels is attributed to different reaction pathways for deoxygenation of the fatty acids and alcohols. To confirm this hypothesis, an experiment with octadecanol was performed. Selectivity to octadecane was stable throughout the reaction being at a level of around 95 % (*Table 4*), which indicates, that the decarboxylation/decarbonylation pathway is more favorable during the transformation of fatty acids.

In addition, experiments with bimetallic 4 % Pt – 4 % Re/TiO_2 were performed. The selectivity to octadecane dropped to a level 82 % at a complete conversion. However, the initial activity doubled even after taking into account the higher metal loading (*Table 4*).

Table 4. Deoxygenation over TiO_2 supported metal catalysts.

Conditions:	Deoxygenation (%)	Initial activity[a]	Selectivity at full conversion of:				
2 MPa			stearic acid (%)			oxygenates (%)	
220 °C			octadecane	heptadecane	octadecanol	octadecane	heptadecane
Stearic acid							
Pt/TiO_2[c]	100	1.11	56	8	36	90	10
(4 MPa)	100	1.68	42	3	55	94	6
(180 °C)	30[e]	0.49	21	2	77	–	–
(Octadecanol)	100	1.44	–	–	–	95	5
Ru/TiO_2[c]	100	1.03	8	77	15	9	91
PtRe/TiO_2[d]	100	1.98[b]	39	15	46	82	18

[a] – initial activity in ($mol_{stearic\ acid} * g_{metal}^{-1} * h^{-1}$); [b] – calculated based on mass of Pt + Re; [c] – 4 % metal loading; [d] – 4 % Pt–4 % Re catalyst; [e] – experiment stopped before complete conversion

3.3.2 Decarboxylation/decarbonylation over Ru/TiO_2 catalyst

The experiment with 4 % Ru/TiO_2 was performed at 220 °C and 2 MPa of total pressure in hydrogen. In contrast to Pt/TiO_2 the main product was heptadecane with selectivity at the end of the reaction 91 %. The reaction pathway follows the formation of aldehyde surface species and its decomposition to CO and (n-1)–hydrocarbon. The fatty acid conversion was slower than over Pt/TiO_2 catalyst, however, only a small amount of octadecanol was formed and the total conversion of oxygenates was faster in the cases of 4 % Ru/TiO_2 (*Table 4*).

The octadecanol yield reached over 20 % at its maximum (*Figure 28*). However, only 9 % of octadecane was formed which indicates that a part of the alcohol undergoes dehydrogenation to aldehyde species.

The proposed mechanism (*Figure 24*) suggests that the main gaseous product of the reaction is CO. However, based on the experimental data it cannot be concluded whether CO or CO_2 were formed as only methane was detected in the gas phase. Methane is a product of the consecutive methanation after the formation of CO_x species.

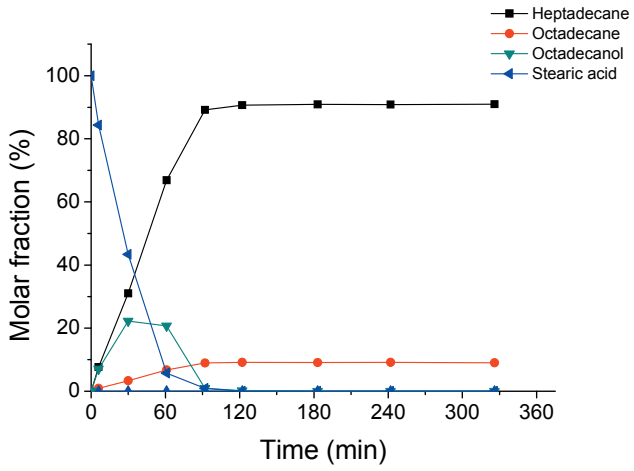

Figure 28. Deoxygenation of stearic acid over 4 % Ru/TiO_2 catalyst at 220 °C in pure hydrogen at 2 MPa of total pressure.

3.3.3 Selective hydrogenation over Re/TiO_2 catalyst

Selective hydrogenation of stearic acid was performed over the 4 % Re/TiO_2 catalyst. The main product was octadecanol (*Figure 29*). The intermediate of the reaction was the aldehyde which is formed at the beginning of the reaction. Moreover, the formation of stearyl stearate was detected after a 10 % conversion of fatty acids. Stearyl stearate is formed from the reaction of stearic acid with octadecanol. The yield of this wax ester was increased with the conversion to reach a maximum at full conversion of stearic acid. Stearyl stearate can be regarded as an intermediate since it can be further converted to the alcohol.

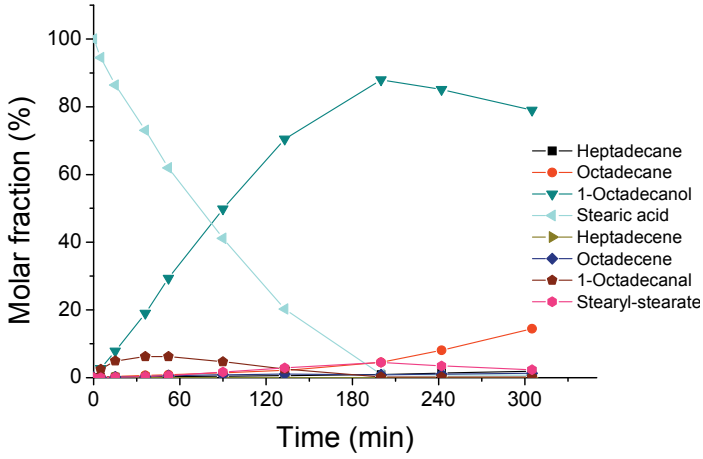

Figure 29. Selective hydrogenation of 0.035 M solution of stearic acid in dodecane over 0.1g 4 % Re/TiO_2 catalyst in pure hydrogen at 2 MPa of total pressure and temperature of 220 °C.

As stearic acid is still present, the main reaction product is octadecanol. However, after a complete conversion of the fatty acid, octadecanol reacts further to form octadecane which is a hydrogenation product of alcohol. Therefore, the catalyst is able to reduce the carboxylic group of the fatty acid to its corresponding alkane. The reason why fatty alcohol did not undergo further transformation in the presence of stearic acid might be the competitive adsorption between the acid and the alcohol. The fatty acid can be adsorbed more strongly on the catalyst surface, therefore, predominantly occupying most of the active sites. With a complete conversion of fatty acid, the alcohol can be adsorbed on the surface and undergo further transformations.

The experiments with 4 % Re/TiO_2 were performed in the temperature range between 180 °C and 220 °C with pure hydrogen used in the gas phase at total pressures between 2 MPa to 4 MPa. The activity of the catalyst was raised with an increase of the temperature and hydrogen pressure where each increment of 1 MPa between 2–4 MPa boosted catalyst activity by 40 % and 30 % respectively (*Figure 30*).

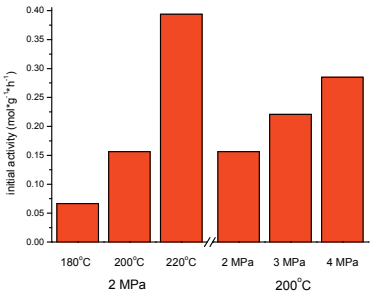

Figure 27. Initial activity of 4% Re/TiO_2 catalyst in reaction with 0.035 M stearic acid diluted in dodecane in ($mol_{stearic\ acid} * g_{Re}^{-1} * h^{-1}$).

The selectivity to octadecanol in all of the experiments was close to 90 % with the highest achieved value of 93 % obtained at 4 MPa and 200 °C (*Figure 31b*). Different selectivities can be thus achieved by manipulation of the reaction temperature and pressure. With a decrease of the temperature, the initial selectivity was higher, which was attributed to a decrease of the initial formation of the aldehyde intermediate at lower conversion levels (*Figure 31a*). Moreover, the selectivity at high conversion levels was slightly increased by the increase of the hydrogen pressure which inhibits the formation of stearyl stearate (*Figure 31b*).

The by–products of the reactions were C_{17} and C_{18} hydrocarbons. The selectivity to these hydrocarbons was higher at the beginning of the experiment and thereafter dropped to a level

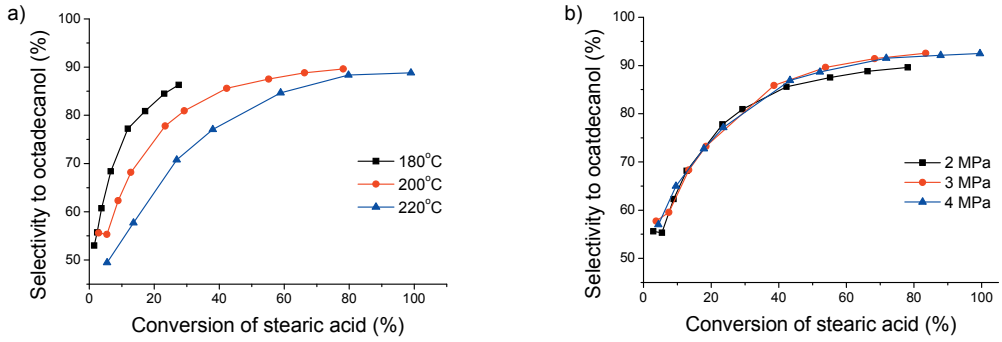

Figure 31. Selectivity to octadecanol vs. conversion of stearic acid in reactions over 4% Re/TiO_2catalyst: a) at different temperatures (180 –220 °C); b) at different total pressure (2–4 MPa)

below 5 %. The initial higher selectivity can be attributed to the induction time for the catalyst. The selectivity to hydrocarbons within the range of 20–80 % in the stearic acid conversion did not change, despite different reaction conditions (*Figure 32*). Furthermore, at an almost complete conversion of stearic acid, the selectivity to hydrocarbons raised again to reach a level of 6 %.

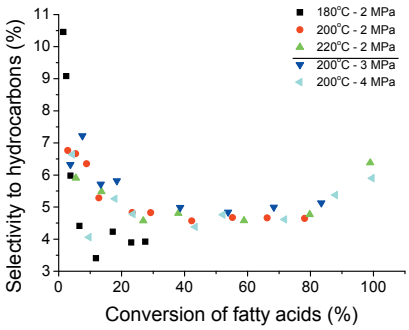

Figure 32. Selectivity to total hydrocarbons vs. conversion of stearic acid in reactions over 4 % Re/TiO_2 catalyst.

While the total amount of hydrocarbons was not influenced by a change of the reaction conditions, the distribution of hydrocarbons was. The main hydrocarbon was octadecane with a fraction of ca. 70 % from all hydrocarbons at the beginning of the reaction. The selectivity for the octadecane formation went through a minimum at medium conversion levels and increased again at complete conversion of stearic acid to ca. 83 %.

Unsaturated C_{18} hydrocarbons were found in the reaction mixture. The selectivity towards octadecenes decreased with an increase of the hydrogen pressure and decrease of the reaction temperature. The C_{17} unsaturated species were found only in the reaction at the highest experientally temperature (220 °C).

As fatty acids were converted, the rate of hydrocarbon formation increased fivefold. Octadecane was the main product with an increasing selectivity as the conversion of octadecanol proceeded.

As mentioned before (*Section 3.1*), rhenium nanoparticles on the support surface were in the form of Re^{4+} and Re^{6+} during the reaction. The experiment with non–reduced 4 % Re/TiO_2 was performed to understand the influence of the rhenium state on the catalytic activity. The initial activity of the non–reduced rhenium catalyst was low 0.07 $(mol_{stearic\ acid} * g_{Re}^{-1} * h^{-1})$ whereas the

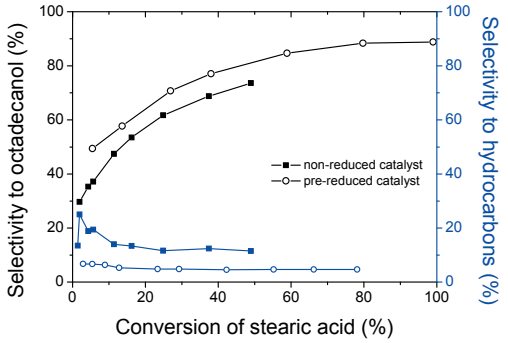

Figure 33. Selectivity to octadecanol (black) and hydrocarbons (blue) vs. conversion of stearic acid in reactions with non-reduced (closed) and pre–reduced (open) 4 % Re/TiO_2 catalyst.

pre–reduced catalyst exhibits an initial activity of 0.39. Moreover, the selectivity to octadecanol was lower with the non–reduced catalyst, and higher formation of hydrocarbons was observed (*Figure 33*). Despite a difference in the conversion and selectivity, the XPS measurements **[VIII]** indicated that the state of rhenium in experiments with both pre–reduced and non–reduced catalysts after the reaction was the same. The pre–reduction of the catalyst is needed for partial reduction of TiO_2 on the interface with rhenium. The Re–Ti^{3+} sites are responsible for formation of alcohol on which the carbonyl group of acids is adsorbed more strongly and thus inhibit further transformation of alcohol to the hydrocarbons. The decrease of the titania oxygen vacancies on the interface with rhenium nanoparticles leading to decrease in the number of sites on which adsorption of acid is strong. Therefore, the alcohol can be more easily transformed to alkanes with the acid still present in the system. It explains both the lower conversion of fatty acids as a number of active sites for the reaction decreased and higher formation of alkanes as the adsorption of alcohol on the catalyst increased. A similar effect was observed with hydrogenation of CO over ReO_x/TiO_2 at 250 °C and 2.1 MPa[42].

4. Conclusions

Extensive studies of fatty acid deoxygenation over Pd/C catalyst were performed to indentify the reaction intermediates and determine the reaction pathways. It was found that in the inert atmosphere, hydrocarbons were produced through decarboxylation of fatty acids yielding CO_2 as the main gas–phase product. However, if hydrogen is introduced to the system, decarbonylation of fatty acids proceeds through formation of aldehyde surface species, which decompose on the palladium surface. Moreover, the fatty alcohol formed over Pd/C catalysts was converted to hydrocarbons predominantly through the dehydrogenation to aldehyde surface species which decomposes to form (n-1)–hydrocarbons. At the same time, the selectivity to n–hydrocarbons through dehydration–hydrogenation reactions was low.

The deoxygenation activity and selectivity of Pd/C catalysts in the reaction with unsaturated fatty acid model compounds decreased with an increase of the fatty acid unsaturation level. The decrease of the selectivity towards linear hydrocarbons in the experiments with unsaturated fatty acids was caused by formation of aromatic by–products originating from unsaturated hydrocarbons by cyclization and subsequent dehydrogenation of the cyclic ring. Moreover, with a low hydrogen content and catalyst metal loading, *cis–trans* isomerization and migration of double bonds occurred at the beginning of the reaction.

The deoxygenation of the industrially available feedstock, tall oil fatty acids was performed over a Pd/C catalyst in a low hydrogen–containing atmosphere (1 %). Similarly to the experiments with model compounds, formation of aromatic species take place which was followed by catalyst deactivation, especially at higher temperatures. It was found that the formation of undesired

species can be inhibited by an increase of the hydrogen partial pressure and catalyst metal loading (4 % Pd), which promotes the hydrogenation of the double bonds in the fatty acids and increase the activity, selectivity and stability of the catalyst. Moreover, pre–hydrogenation of the feedstock at 120 °C over Pd/C increased the selectivity towards hydrocarbons to 95 % which was stable throughout the reaction.

The deoxygenation of stearic acid, ethyl stearate and technical tristearin was performed in a fixed bed reactor over egg–shell Pd/C beads. The stearic acid conversion was stable under the 5 % H_2/Ar gas atmosphere. However, in the experiments with the prolonged time on stream, the activity of the catalyst decreased with time which was caused by the formation of carbon deposits on the catalyst surface. Moreover, with an inert gas atmosphere, catalyst deactivation was observed for all feedstock.

New catalyst materials were proposed for the deoxygenation of fatty acids. The use of TiO_2 supported metal catalysts allowed to decrease the process temperature by ~100 °C. Moreover, by introducing different metals onto TiO_2, selectivity to the desired products can be tuned. The deoxygenation over Ru/TiO_2 catalyst occurred mainly though decarboxylation/decarbonylation of stearic acid to (n-1)–carbon heptadecane. Deoxygenation over Pt/TiO_2 catalyst occurred through full hydrogenation of the carboxylic group to yield corresponding hydrocarbon – octadecane. Moreover, the selectivity to octadecane was enhanced by an increase of the hydrogen partial pressure or a decrease of the temperature.

The new method for selective hydrogenation of fatty acid to corresponding alcohols was proposed over ReO_x/TiO_2 catalysts. Stearic acid was converted to octadecanol with a selectivity up to 93 %. A consecutive reaction of the alcohol to the corresponding alkane was inhibited by competitive adsorption of the acid and the alcohol, in which the first has a higher affinity towards the catalyst surface. After a complete conversion of fatty acids, the fatty alcohol can be further transformed to hydrocarbons, predominantly through dehydration–hydrogenation.

5. Notation

DCO – Decarboxylation/Decarbonylation

FAME – Fatty Acids Methyl Esters

HDO – Hydrodeoxygenation

ICP–OES – Inductively Coupled Plasma – Optical Emission Spectroscopy

LA–ICP–MS – Laser-Ablation Inductively Coupled Plasma Mass Spectrometry

LT-ELS – Low Temperature Evaporative Light Scattering Detector

OECD – Organization for Economic Co-operation and Development

OPEC – Organization of the Petroleum Exporting Countries

RON – Research octane number

TEM – Transmission Electron Microscopy

TOF – Turnover Frequency

TOFA – Tall Oil Fatty Acids

TOS – Time–on–stream

TPD – Temperature Programmed Desorption

TPR – Temperature Programmed Reduction

XPS – X-Ray Photoelectron Spectroscopy

XRD – X-Ray Diffraction

6. References

[1] OPEC, *Annual Statistical Bulletin 2013*, **2013**.
[2] U.S. Energy Information Administration (EIA), *Short-Term Energy and Summer Fuels Outlook (STEO)*, **2014**.
[3] BP, *BP Energy Outlook 2035*, **2014**.
[4] E. E. Commission, *Off. J. Eur. Union Belgium* **2009**, 16–62.
[5] *Annual Report 2013 – Neste Oil*, **2013**.
[6] P. Priecel, L. Čapek, D. Kubička, F. Homola, P. Ryšánek, M. Pouzar, *Catal. Today* **2011**, *176*, 409–412.
[7] P. Priecel, D. Kubička, L. Čapek, Z. Bastl, P. Ryšánek, *Appl. Catal. A Gen.* **2011**, *397*, 127–137.
[8] J. Walendziewski, M. Stolarski, R. Łużny, B. Klimek, *Fuel Process. Technol.* **2009**, *90*, 686–691.
[9] J. Monnier, H. Sulimma, A. Dalai, G. Caravaggio, *Appl. Catal. A Gen.* **2010**, *382*, 176–180.
[10] M. Toba, Y. Abe, H. Kuramochi, M. Osako, T. Mochizuki, Y. Yoshimura, *Catal. Today* **2011**, *164*, 533–537.
[11] D. C. Elliott, T. R. Hart, G. G. Neuenschwander, L. J. Rotness, A. H. Zacher, *Environ. Prog. Sustain. Energy* **2009**, *28*, 441–449.
[12] S. Bezergianni, A. Dimitriadis, *Renew. Sustain. Energy Rev.* **2013**, *21*, 110–116.
[13] M. M. Ahmad, M. Fitrir, R. Nordin, M. T. Azizan, *Am. J. Appl. Sci.* **2010**, *7*, 746–755.
[14] D. Kubička, J. Horáček, *Appl. Catal. A Gen.* **2011**, *394*, 9–17.
[15] P. Šimáček, D. Kubička, G. Šebor, M. Pospíšil, *Fuel* **2010**, *89*, 611–615.
[16] I. Kubičková, D. Kubička, *Waste and Biomass Valorization* **2010**, *1*, 293–308.
[17] E.-M. Ryymin, M. L. Honkela, T.-R. Viljava, O. I. Krause, *Appl. Catal. A Gen.* **2009**, *358*, 42–48.
[18] M. Krár, S. Kovács, D. Kalló, J. Hancsók, *Bioresour. Technol.* **2010**, *101*, 9287–93.
[19] O. Şenol, T.-R. Viljava, O. I. Krause, *Catal. Today* **2005**, *106*, 186–189.
[20] O. Şenol, T.-R. Viljava, O. I. Krause, *Appl. Catal. A Gen.* **2007**, *326*, 236–244.
[21] D. Kubička, L. Kaluža, *Appl. Catal. A Gen.* **2010**, *372*, 199–208.
[22] J. G. Immer, M. J. Kelly, H. H. Lamb, *Appl. Catal. A Gen.* **2010**, *375*, 134–139.
[23] E. W. Ping, R. Wallace, J. Pierson, T. F. Fuller, C. W. Jones, *Microporous Mesoporous Mater.* **2010**, *132*, 174–180.
[24] P. Mäki-Arvela, I. Kubickova, M. Snåre, K. Eränen, D. Murzin, *Energy & Fuels* **2007**, *21*, 30–41.
[25] M. Snåre, I. Kubičková, P. Mäki-Arvela, D. Chichova, K. Eränen, D. Y. Murzin, *Fuel* **2008**, *87*, 933–945.

[26] S. Lestari, P. Mäki-Arvela, I. Simakova, J. Beltramini, G. Q. M. Lu, D. Y. Murzin, *Catal. Letters* **2009**, *130*, 48–51.
[27] M. Snåre, I. Kubickova, P. Mäki-Arvela, K. Eränen, D. Y. Murzin, *Ind. Eng. Chem. Res.* **2006**, *45*, 5708–5715.
[28] S. Lestari, J. Beltramini, G. Lu, *Stud. Surf. Sci. Catal.* **2008**, *174*, 1339–1342.
[29] O. V. Kikhtyanin, A. E. Rubanov, A. B. Ayupov, G. V. Echevsky, *Fuel* **2010**, *89*, 3085–3092.
[30] B. Peng, X. Yuan, C. Zhao, J. A. Lercher, *J. Am. Chem. Soc.* **2012**, *134*, 9400–5.
[31] T. Turek, D. L. Trimm, N. W. Cant, *Catal. Rev.* **1994**, *36*, 645–683.
[32] C. Boswell, *Detergent Alcohols Growing Capacity Will Continoue to Drive down Operating Rates*, **2013**.
[33] J. Carnahan, T. Ford, *J. Am. Chem. Soc.* **1955**, *77*, 3766–3768.
[34] M. Toba, S. Tanaka, S. Niwa, *Appl. Catal. A Gen.* **1999**, *189*, 243–250.
[35] M. . Mendes, O. Santos, E. Jordão, A. . Silva, *Appl. Catal. A Gen.* **2001**, *217*, 253–262.
[36] H. G. Manyar, C. Paun, R. Pilus, D. W. Rooney, J. M. Thompson, C. Hardacre, *Chem. Commun.* **2010**, *46*, 6279–81.
[37] K. Yoshino, Y. Kajiwara, N. Takaishi, Y. Inamoto, J. Tsuji, *J. Am. Oil Chem. Soc.* **1990**, *67*, 21–24.
[38] T.-S. Tang, K.-Y. Cheah, F. Mizukami, S. Niwa, M. Toba, Y.-M. Choo, *J. Am. Oil Chem. Soc.* **1993**, *70*, 601–605.
[39] P. a. Simonov, S. Y. Troitskii, V. a. Likholobov, *Kinet. Catal.* **2000**, *41*, 255–269.
[40] O. Simakova, P. Simonov, A. Romanenko, I. Simakova, *React. Kinet. Catal. Lett.* **2008**, *95*, 3–12.
[41] S. Lestari, P. Maki-Arvela, H. Bernas, O. Simakova, R. Sjöholm, J. Beltramini, G. Q. M. Lu, J. Myllyoja, I. Simakova, D. Y. Murzin, *Energy & Fuels* **2009**, *23*, 3842–3845.
[42] M. Komiyama, J. Sato, K. Yamamoto, Y. Ogino, *Langmuir* **1987**, *3*, 845–851.
[43] J. Okal, *Appl. Catal. A Gen.* **2005**, *287*, 214–220.
[44] D. Murzin, I. Kubickova, M. Snåre, P. Mäki-Arvela, J. Myllyoja, *Method for the Manufacture of Hydrocarbons, US 7491858*, **2009**.
[45] V. F. Surovikin, G. V Plaxin, V. A. Semikolenov, V. A. Likholobov, I. J. Tiunova, *Porous Carbonaceous Material, US 4978649*, **1990**.
[46] J. Tsuji, K. Ohno, *J. Am. Chem. Soc.* **1968**, *61*, 94–98.
[47] K. Fujimoto, T. Kunugi, *Appl. Catal.* **1987**, *29*, 203–210.
[48] J. Davis, M. Barteau, *Surf. Sci.* **1990**, *235*, 235–248.
[49] H. Bernas, K. Eränen, I. Simakova, A.-R. Leino, K. Kordás, J. Myllyoja, P. Mäki-Arvela, T. Salmi, D. Y. Murzin, *Fuel* **2010**, *89*, 2033–2039.
[50] I. Simakova, O. Simakova, P. Mäki-Arvela, D. Y. Murzin, *Catal. Today* **2010**, *150*, 28–31.
[51] J. G. Immer, H. H. Lamb, *Energy & Fuels* **2010**, *24*, 5291–5299.

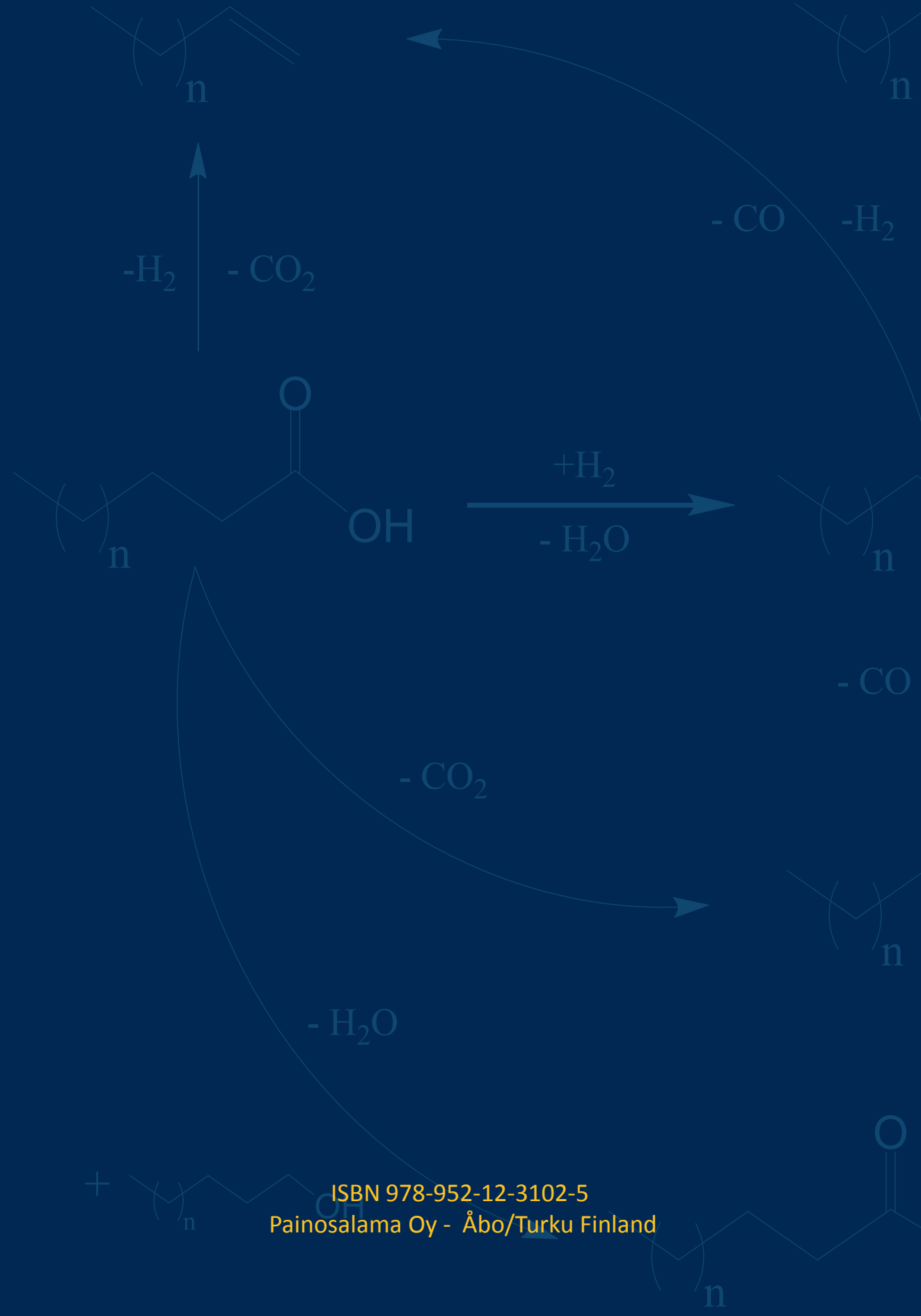

ISBN 978-952-12-3102-5
Painosalama Oy - Åbo/Turku Finland